Pacific Northwest
NATIONAL LABORATORY

PNNL-30105, Rev. 0
RPT-OSIF-012, Rev. 0

Iodine Speciation Basis and Gap Analysis for Hanford Tank Farm Inventory and during Processing

August 2020

RM Asmussen
TG Levitskaia
CL Bottenus
MS Fountain

U.S. DEPARTMENT OF ENERGY

Prepared for the U.S. Department of Energy
under Contract DE-AC05-76RL01830

DISCLAIMER

PACIFIC NORTHWEST NATIONAL LABORATORY
operated by
BATTELLE
for the
UNITED STATES DEPARTMENT OF ENERGY
under Contract DE-AC05-76RL01830

Printed in the United States of America

Available to DOE and DOE contractors from the
Office of Scientific and Technical Information,
P.O. Box 62, Oak Ridge, TN 37831-0062;
ph: (865) 576-8401
fax: (865) 576-5728
email: reports@adonis.osti.gov

Available to the public from the National Technical Information Service
5301 Shawnee Rd., Alexandria, VA 22312
ph: (800) 553-NTIS (6847)
email: orders@ntis.gov <https://www.ntis.gov/about>
Online ordering: http://www.ntis.gov

PNNL-30105, Rev. 0
RPT-OSIF-012, Rev. 0

Iodine Speciation Basis and Gap Analysis for Hanford Tank Farm Inventory and during Processing

August 2020

RM Asmussen
TG Levitskaia
CL Bottenus
MS Fountain

Prepared for
the U.S. Department of Energy
under Contract DE-AC05-76RL01830

Pacific Northwest National Laboratory
Richland, Washington 99354

Summary

Pacific Northwest National Laboratory (PNNL) is providing baseline technical support to Washington River Protection Solutions, LLC, for the Flowsheet Integration team. This report documents the evaluation of the technical bases available to support iodine speciation and distribution within Hanford wastes and subsequent waste streams generated during Direct Feed Low-Activity Waste pretreatment operations – specifically, waste retrievals, evaporation, and feed staging, as well as particle filtration and cesium decontamination using crystalline silicotitanate (CST) ion exchange [in the Tank Side Cesium Removal (TSCR) system].

Predicting and tracking iodine speciation, associated glass retention, subsequent splits in the Hanford Waste Treatment and Immobilization Plant (WTP) low-activity waste (LAW) primary and secondary off-gas systems, behavior during evaporation in the Effluent Management Facility (EMF) and treatment in the Effluent Treatment Facility (ETF) will contribute toward mitigating regulatory and flowsheet risks during the direct feed low-activity waste (DFLAW) mission and beyond. However, the technical basis for iodine speciation predictions throughout the Hanford flowsheet is poorly documented and highly presumptive. Iodine speciation in the tank waste is currently assumed, based on historic PUREX process knowledge, to be predominantly iodide (I^-) with only small fractions of iodate (IO_3^-) and organoiodine and has not been confirmed. These assumptions do not consider redox and chemical transformations of iodine which occur during decades-long storage of the tank waste, resulting in potentially incorrect technical conclusions about feed iodine speciation and subsequent behavior. The consequences of not confirming the assumptions of iodine speciation are the use of inappropriate iodine surrogates (e.g., potassium iodide) and their concentrations in non-radiological unit operations testing which forms the basis for all iodine decontamination factors (DFs) in DFLAW flowsheet modeling; and the inability to validate and project iodine speciation and behavior across the flowsheet.

This report represents a first-of-its-kind, thorough interrogation of the factors controlling iodine speciation in Hanford tank wastes, both in the tank and during its movement through the flowsheet up to WTP. The information within this report can be used to direct efforts to close crucial technical gaps and better project iodine behavior at Hanford. PNNL performed a literature survey of information related to iodine species in environments analogous to Hanford tank waste and the subsequent waste streams to define a technical basis for the possible iodine speciation in Hanford waste. In doing so, the relevancy of past and future laboratory studies can be assessed and anticipated, respectively, for demonstrating unit operation performance and establishing flowsheet modeling bases related to to changing iodine speciation across the Hanford tanks. The task evaluated iodide and iodate as the primary species of interest, with a focus on organo-iodine where appropriate.

The analysis identified several technical gaps and opportunities related to iodine speciation and the associated impacts in the flowsheet. These can be summarized in four major themes:

1. The available literature lacks information defining the behavior of iodine species under the high ionic strength (e.g. > 5 mol/L Na), alkalinity (pH > 12) and radiation environment typical for Hanford wastes.

2. There is little data available on the influence of radiolysis on iodine speciation within the tanks to make an assessment for Hanford-relevant conditions. While iodine speciation is speculated to be stable – iodide being the majority with a fraction of iodate based on processing history – decades of irradiation may have altered this projected ratio. It is speculated that the concentration of iodine in the supernatant may play a substantial role in its radiolytic transformations, but quantitative data are largely lacking. The gap is further complicated by the unknown role of organic species, especially in complexant tanks. A focused testing effort can close this technical gap.

3. Expanded characterization of the saltcake and sludge is required to validate assumptions of iodine inventory in these phases and identify the associated iodine species. This is integral to confirming the projected iodine content in the waste feeds to the Hanford Waste Treatment and Immobilization Plant (WTP) and accurately representing solubility that determines wash factors for each waste phase.

4. The influence of speciation on differing unit operations is somewhat speculative without supporting data. Iodine speciation can dictate partitioning in the various unit operations and influence downstream units. Testing in representative operation conditions, with actual waste and/or surrogates at appropriate concentrations, would be required to close this knowledge gap.

These technical gaps and opportunities were drawn from a combination of literature review summaries of chemical and environmental influences on iodine speciation, Hanford iodine inventory accounting across the tank farms, chemical marker correlations in the tanks and waste feed to the WTP LAW Facility, and flowsheet evaluations. A similar exercise to evaluate iodine speciation from the melter through to ETF should be performed to expand on preliminary evaluations[1]. Additional findings of note include:

- While both iodide and iodate are expected to be stable in the expected tank conditions, radiolysis is likely to influence speciation and deviate from the expected ratios, which also can depend on the total iodine concentration in the waste.
- Sampling data used to verify iodine inventory are most widely available for the supernatant in double-shell tanks but are lacking for other waste phases.
- A significant iodine inventory is present in the complexant tanks – primarily in the AN farm – where behavior may differ from the other farms due to the presence of organic complexants and other organic compounds in these tanks.
- The presence of I-127 needs to be better documented outside of the nine tanks currently measured.
- Iodine is most correlated with technetium and sodium within the tank wastes, with the strongest correlations present in the supernatant.
- Many assumptions are used to predict iodine partitioning, which may be dictated by speciation, throughout the Hanford flowsheet and within TOPSim[2].
- During retrievals, dilution will occur and is not likely to induce a speciation change during processing as dilution was only determined to influence radiolysis products over long periods.
- During evaporation, iodide and iodate are projected to remain in the concentrate, while organo-iodine species may differ in partitioning and stability based on the behavior of other volatile organics in evaporator testing.
- Iodine shows concentration correlations with Cs, Tc, Cl, NO_3^-/NO_2^- ratio, and oxalate (inverse correlation) in the feed vector to the TSCR system.
- Filtration will not impact iodine speciation but may remove the iodine fraction trapped in the filtered-out particulates.
- Some species (Pb, Hg, Sr, Ca) that become bound to CST can interact and form low-solubility species with iodine and may lead to iodine retention during ion exchange.

[1] Fountain MF, TG Levitskaia and RM Asmussen. 2019. *Iodine Speciation and Flowsheet Inventory Tracking Gaps in DFLAW Flowsheet.* LTR-OSIF-007. Pacific Northwest National Laboratory, Richland, WA (not publicly available)

[2] TOPSim is a software application used to host and simulate models of the Hanford tank farms and processing plant operations (see Bernards et al. 2018).

Acknowledgments

The authors would like to thank Washington River Protection Solutions, LLC, for project support, specifically, Jacob Reynolds for project guidance and Laura Cree for data sharing. The authors also wish to thank Philip Schonewill and Stuart Arm for their technical reviews, William Dey for Quality Assurance and Matt Wilburn for the technical editing. We thank Richard Daniel for calculation reviews and Richard Cox for data management. We thank Michael Stone for peer review.

Acronyms and Abbreviations

BBI	Best Basis Inventory
BNFL	British Nuclear Fuels Limited
BNI	Bechtel National, Inc.
C	direct calculation
CST	crystalline silicotitanate
DFLAW	Direct Feed Low-Activity Waste
DST	double-shell tank
E	process knowledge
E_h	reduction potential
EMF	Effluent Management Facility
ETF	Effluent Treatment Facility
GAC	granular activated carbon
HLW	high-level waste
HTWOS	Hanford Tank Waste Operations Simulator
IDF	Integrated Disposal Facility
ILAW	immobilized low-activity waste
LAW	low-activity waste
LAWPS	Low-Activity Waste Pretreatment System
LDR	land disposal restriction
LERF	Liquid Effluent Retention Facility
LSW	liquid secondary wastes
NOM	natural organic matter
OD	other debris
PA	performance assessment
PNNL	Pacific Northwest National Laboratory
PUREX	Plutonium Uranium Extraction
QA	quality assurance
R&D	research and development
S	direct sampling
SBS	submerged bed scrubber
SST	single-shell tank
SSW	solid secondary waste
TE	model-based template estimate
TOC	Tank Operations Contractor
TS	sample case template estimate
TSCR	Tank Side Cesium Removal

TWINS	(Hanford) Tank Waste Information Network System
WESP	wet electrostatic precipitator
WRPS	Washington River Protection Solutions, LLC
WTP	Hanford Waste Treatment and Immobilization Plant
WVR	waste volume reduction
WWFTP	WRPS Waste Form Testing Program

Contents

Figures

Tables

1.0 Introduction

1.1 Background

Pacific Northwest National Laboratory (PNNL) is providing baseline technical support to Washington River Protection Solutions, LLC (WRPS) for the Flowsheet Integration team. Predicting and tracking iodine speciation, associated glass retention, subsequent splits in the Hanford Waste Treatment and Immobilization Plant (WTP) low-activity waste (LAW) primary and secondary off-gas systems, behavior during evaporation in the Effluent Management Facility (EMF) and treatment in the Effluent Treatment Facility (ETF) will contribute toward mitigating regulatory and flowsheet risks. However, the technical basis for iodine speciation predictions throughout the Hanford flowsheet are poorly documented and highly presumptive. This report documents the evaluation of the technical basis available to support iodine speciation information within Hanford wastes and subsequent waste streams generated during DFLAW operations. PNNL performed a literature survey of information related to iodine species in environments analogous to Hanford waste to define a technical basis for the possible iodine speciation in Hanford waste. Doing so can determine the likelihood of laboratory studies on iodine speciation in tank waste being universally relevant across the Hanford tanks. The task evaluated iodide, iodate, and organo-iodine as the primary species of interest.

To date little has been reported on the speciation of iodine in the Hanford tanks, and it has been presumed to be a mixture of thermodynamically stable iodide and iodate. There are many chemical and environmental factors that could dictate iodine speciation, including pH, reduction potential (E_h), radiolysis, solubilities, and organics present. The underlying fundaments of how each of these factors influences iodine speciation are presented in the report. Based on this understanding and the known inventory and distribution of iodine at Hanford, this report discusses the iodine speciation considerations and impacts at each unit operation from the SSTs through to the ion exchange unit operation within the Tank Side Cesium Removal (TSCR) system.

The currently adopted assumptions of iodine behavior directs experimental conditions to evaluate specific unit operation and waste form qualification testing. For example, based on prior reports the species of iodine used in waste form testing is iodide. However, as covered in this report conditions exist that would favor the presence of iodate. As well, in pretreatment operations the assumption has been only iodide is present and speciation would not impact partitioning and behavior through the pretreatment unit operations.

Iodine speciation in the waste upon delivery to the WTP LAW Facility may influence its behavior and partitioning, beginning with how much iodine is retained in the glass versus discharged to the off-gas system. The different species of iodine have different volatilities, dictating their behavior in the melter plenum, and differing oxidation states (e.g., I^{5+} for iodate, IO_3^-; I^{1-} for iodide, I^-; and I^0 for elemental iodine, I_2) that respond differently to the oxidizing conditions of the melter cold cap. Gaseous I_2 is observed to be emitted from the melter when iodide (as potassium iodide) is added to the melter feed. This speciation in WTP operations is likely dictated by the iodine speciation originating in the tanks and moving through the flowsheet. Thus, the focus of this report is on the speciation of iodine up to WTP. A similar evaluation of iodine speciation moving through WTP and toward end state disposal should be performed. The impact of iodine speciation moving downstream from the melter is discussed in brief below, although not fully detailed in this report.

The speciation of iodine moving to the off-gas system may be dictated by the nature of individual iodine species in the melter. This resulting gas phase speciation may affect the affinity of iodine for the submerged bed scrubber (SBS) and wet electrostatic precipitator (WESP). The two species that have been

primarily observed to be emitted from the melter are HI gas and I_2 gas (Deng et al. 2016), with ICl, I_2, NOI, and other iodine species possible. HI gas would be expected to be readily removed by the SBS because it is an acid gas adsorbing into a neutral pH solution. I_2 gas, however, must undergo simultaneous hydrolysis and disproportionation to be removed by the SBS or WESP[3]. Thus, the speciation of iodine fed to the melter (which is poorly known) may determine behavior and speciation evolving from the melter, especially in the case of organo-iodine. Recent work has highlighted the discrepancy between iodide, iodate and organo-iodine behavior in the melter (Matlack et al. 2020). The species evolved from the melter determine how much iodine is captured by the WESP and SBS and influencing how iodine will behave further downstream. In turn, this behavior will directly impact the iodine distribution across waste form types destined for the Integrated Disposal Facility (IDF). Iodine release from a glass waste form in the IDF would be expected to be lower than from an un-amended grout (Bates et al, 2019).

Recent scrutiny has been placed on the amount of iodine sorbed on the carbon adsorber bed. A WTP presentation[4] presented results from a Vitreous State Laboratory experimental report indicating that iodine removal efficiency in the WTP LAW Facility off-gas carbon beds degraded from greater than 99% during initial operation to 74% after only 33 hours of run time. This result is much less than the expected 99% retention assumed in flowsheet modeling and indicates that over the expected carbon bed service period of two years (Tranbarger 2018), any iodine retention credit placed on the carbon bed carries significant risk without additional data. The level of sorption in the carbon bed depends on the iodine species in the gas phase, the concentration arriving at the carbon bed (including both the I-129 and I-127 isotopes the ratio of which is uncertain) and the presence of other species such as NO_x that drastically affect sorption retention (Vienna 2015). Previous testing efforts have sent higher concentrations of contaminants than expected to the carbon bed in scaled testing.

Downstream from the carbon bed, the caustic scrubber can remove iodine gas for air permit compliance, if necessary, but requires alkaline pH to do so. Given that it is unknown how much iodine will partition to the melter, SBS, WESP, TCO, and carbon beds, it is also unknown what is the appropriate operating pH for the caustic scrubber in order to remove the rest of the iodine prior to discharge of the off-gas to the atmosphere. The pH profile (continually adjusted to a target value with NaOH additions) of the caustic scrubber is currently determined by how much CO_2, Cl_2, HCl, and NOx is absorbed from the off-gas and no consideration given for iodine absorption. Determining the right pH to balance process objectives is important since these chemical species can directly influence the amount of brine produced at the Effluent Treatment Facility (ETF), because the ETF receives the caustic scrubber effluent in a combined stream with the Effluent Management Facility (EMF) process condensate.

1.2 Report Contents

To build a technical foundation to understand iodine speciation at Hanford and assist in interpreting the universality of upcoming iodine speciation measurements, the open literature, Hanford reports, and databases were reviewed for the following purposes:

- Document the foundational chemical and environmental factors that could influence iodine speciation in Hanford-relevant conditions.

[3] Fountain MF, TG Levitskaia and RM Asmussen. 2019. *Iodine Speciation and Flowsheet Inventory Tracking Gaps in DFLAW Flowsheet.* LTR-OSIF-007. Pacific Northwest National Laboratory, Richland, WA (not publicly available)

[4] PowerPoint presentation from Robert Hanson (Bechtel National Inc.) and Brad Stiver (Bechtel National Inc.) titled, “LAW Offgas System Iodine 129 Removal.” No presentation date provided. File properties provide 12/4/2018 as “last modified” date.

- Evaluate the Hanford tank waste inventory and distribution of iodine categorized by waste phase (sludge, saltcake, and supernatant), by tank type [double-shell tanks (DSTs), single-shell tanks (SSTs), tank farms containing complexant tanks], and by known isotopic quantities of iodine.
- Identify where iodine sampling has been completed and how sampling data correlate to projections from the various sample bases used.
- Evaluate the relationship between iodine and other waste constituents in both the Hanford tank waste and the LAW feed to the WTP LAW Facility.
- Evaluate the possibilities for iodine speciation changes during tank retrieval, staging, and pretreatment (i.e., effects of dilution, evaporation, temperature, pH).
- Identify outstanding flowsheet gaps in iodine speciation.

1.3 Report Organization

The technical discussion begins in section 3.0 and presents a review of the fundamental chemistry and environmental conditions that can influence iodine speciation in Hanford-relevant conditions. Section 4.0 presents the inventory of I-129 in Hanford tank waste based on Best Basis Inventory (BBI)[5] data and provides an accounting of the inventory by tank type, waste phase, and isotopic ratios. Section 5.0 discusses previously documented projections of iodine speciation in the tanks, along with chemical marker correlations between iodine and elements of interest within the tanks, that can influence or infer iodine speciation. Section 6.0 summarizes the basis and assumptions from the perspective of the flowsheet: what is known or expected from Hanford tank waste history and processing assumptions, what is applied to the flowsheet modeling, and gaps that exist. This section bridges the understanding between what is known to be in tank farms and what is expected to happen to iodine during DFLAW processing by discussing the key parameters that impact iodine speciation. Section 7.0 discusses the impact of DFLAW tank retrieval activities and pretreatment processes on iodine speciation and presents chemical marker correlations between iodine and elements of interest in the LAW feed following filtration and ion exchange. Lastly, section 8.0 discusses conclusions that can be drawn and gaps in the available information, with recommendations to close these identified technical gaps.

[5] The Best Basis Inventory is a database of best-basis inventory estimates for chemical and radionuclide components in the 177 Hanford Site underground storage tanks.

2.0 Quality Assurance

This work was conducted with funding from WRPS under PNNL project 75807, contract 36437-301, with the title “Flowsheet Maturation Activities.”

All research and development (R&D) work at PNNL is performed in accordance with PNNL’s Laboratory-level Quality Management Program, which is based on a graded application of NQA-1-2000, *Quality Assurance Requirements for Nuclear Facility Applications* (ASME 2000), to R&D activities. To ensure that all client quality assurance (QA) expectations were addressed, the QA controls of the WRPS Waste Form Testing Program (WWFTP) QA program were also implemented for this work. The WWFTP QA program implements the requirements of NQA-1-2008, *Quality Assurance Requirements for Nuclear Facility Applications* (ASME 2008), and NQA-1a-2009, *Addenda to ASME NQA-1-2008* (ASME 2009), and consists of the WWFTP Quality Assurance Plan (QA-WWFTP-001) and associated procedures that provide detailed instructions for implementing NQA-1 requirements for R&D work.

The work described in this report was assigned the technology level “Applied Research” and was planned, performed, documented, and reported in accordance with procedure QA-NSLW-1102, *Scientific Investigation for Applied Research*. All staff members contributing to the work received appropriate technical and QA training prior to performing quality-affecting work.

3.0 Chemical and Environmental Influences on Iodine Speciation

3.1 Chemical Parameters

Iodine speciation, in the context of DFLAW-relevant process conditions, is discussed below based on open literature and fundamental iodine chemistry arguments. While iodine can exist in oxidation states ranging from -1 to +7 , the most stable valence states and corresponding chemical species in solution include -1 (iodide, I^-), 0 (elemental iodine, I_2), combination of –1 and 0 (triiodide, I_3^-), +1 (hypoiodite, IO^-), +5 (iodate, IO_3^-), and +7 (periodate, IO_4^- or orthoperiodate, $H_3IO_6^{2-}$). For alkaline solutions, redox processes of iodine are described by the Latimer diagram (Figure 3.1), suggesting that iodate and iodide are the most stable iodine species (Latimer 1952).

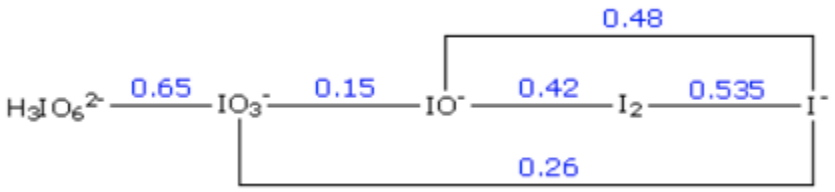

Figure 3.1. Latimer diagram of standard reduction potentials for iodine in aqueous basic solutions. The potentials are given in volts relative to standard hydrogen electrode per one electron process. Adapted from Latimer (1952).

This behavior is consistent with the aqueous iodine speciation based on a classical chemical equilibrium E_h–pH diagram of iodine for the aerated systems (Doizi 2012). Interestingly, iodate steadily becomes more favorable as pH increases (Figure 3.2, left pane), so it is a thermodynamically stable iodine species at very high concentrations of free hydroxide typical of Hanford tank waste. The speciation diagram predicts iodide and iodate to be the only aqueous stable iodine species at high pH (Figure 3.2, right pane). The Hanford tanks are kept alkaline with targeted chemistry to maintain integrity of the carbon-steel tank walls. The ratio of nitrate/nitrite is adjusted based on the hydroxide concentration to maintain corrosion redox conditions (Beavers et al. 2014; Uytioco 2019). Traditionally the E_h–pH diagram would be used to determine likely speciation by measuring the E_h and pH respectively to identify the species at those conditions. However, direct measurements of the E_h of the tanks is extremely challenging due to the redox disequilibrium in the tanks and multiple competing reaction. While such a measurement in future tank sampling efforts would be valuable to assist in speciation determination, the measurement and interpretation would be difficult. As such, a series of environmental factors within the tanks can also be considered to predict iodine speciation and are discussed below.

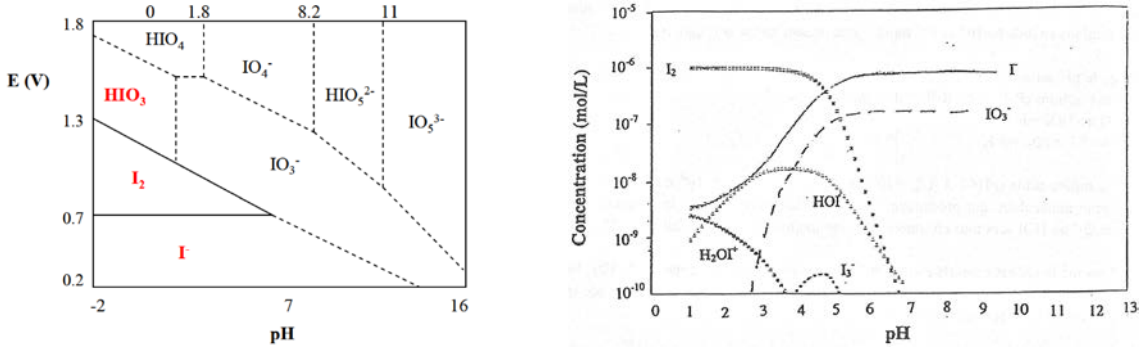

Figure 3.2. E_h-pH diagram (left pane) and representative speciation diagram (right pane, 1 µM total iodine) of aqueous iodine. Adapted from Doizi (2012), https://cetama.partenaires.cea.fr/Local/cetama/files/481/04Doizi31-05-2012.pdf.

Elemental iodine readily hydrolyses at pH above about 6, initially forming hypoiodic acid, HIO, which will rapidly disproportionate into iodide and iodate. The ionization constant of HIO is 2.3×10^{-11} (Chia 1958) and the corresponding pK_a value is 10.6, meaning that at pH 10.6 half of the HIO deprotonates to IO^-, and at pH 12 and above exists as IO^-. Therefore, in highly alkaline solutions typical of the Hanford tank waste, the major processes of elemental iodine hydrolysis and hypoiodite disproportionation into the final iodate and iodide products can be expressed by the simplified reactions in Eqs. (3.1) through (3.3), albeit many different composition-dependent molecular mechanisms are possible. Complex I_3^- species are excluded from the discussion herein because they have been shown to be unimportant at iodine concentrations lower than 1 mM (Truesdale et al. 1994) and significantly lower iodine concentrations are expected in the Hanford supernatants. Neither I_2 nor IO^- is expected to be present in highly alkaline solutions. However, they play an important role as intermediates in the redox chemistry of iodine, which is complex, multi-pathway, and matrix-dependent (Zhang and Hou 2013).

$$I_2 + 2OH^- \rightarrow I^- + IO^- + H_2O \quad (3.1)$$

$$3IO^- \rightarrow 2I^- + IO_3^- \quad (3.2)$$

$$3I_2 + 6OH^- \rightarrow 5I^- + IO_3^- + 3H_2O \quad (3.3)$$

Truesdale et al. (1994) evaluated disproportionation of HIO/IO^- into iodide and iodate in alkaline solutions and observed that the disproportionation mechanism progressively changes as pH increases from 7 and 13, which was attributed to additional reactions involving and I_2OH^- intermediate species when pH is greater than 10. The presence of this species explained the lack of a reciprocal dependence of the reaction rate on hydroxyl (OH^-) concentration observed in highly alkaline solutions; the maximum rate of disproportionation was found at pH between 9 and 10 and decreased at pH 11 and higher. Inclusion of the I_2OH^- species in the model supported a previously documented first-order dependence with respect to iodide concentration (Wren et al. 1986). This implies that intermediate IO^- is relatively more stable in highly alkaline solutions at a given total iodine concentration in the system providing time for 1) its further oxidation to iodate and 2) reaction with organics if present in the system.

This conclusion agrees with a previous report that studied kinetics of HIO disproportionation in borate and carbonate buffers at pH range 7.6 to 11 (Bichsel and Von Gunten 2000). The objectives of their study were to quantify the catalytic effect of buffers on disproportionation of HIO and assess kinetic competition of HIO disproportionation to iodate and iodide with other transformations, including its oxidation to iodate and reaction with natural organic matter (NOM). They determined that even though

buffers significantly accelerate HIO disproportionation, it remains slow, and the half-life of HIO ranges from 10 to 1000 days under typical drinking water conditions. Under their experimental conditions, the initial half-life was never lower than approximately 2 days. They concluded that the dominating processes are HIO's further oxidation to iodate and reaction with NOM leading to formation of organo-iodine compounds. It is feasible that a similar mechanism could occur within tank waste with similar organic functional groups as HIO is expected to be generated as transient species during redox interconversion of I- during radiolysis-driven processes, leading to formation of organoiodine species due to HIO reaction with similar organic functional groups.

The direct oxidation of iodide by ozone (O_3) is well established. Under acidic conditions, I_2 is the main reaction product while formation of iodate dominates under neutral and alkaline conditions (Parry and Hern 1973). For instance, Bichsel and Von Gunten (1999) reported that during oxidative water treatment with O_3, iodide oxidizes to iodate rapidly (within 1 second) with HIO being a transient species. Atmospheric and aqueous iodide plays a major role in ozone tropospheric ozone catalytic destruction, and theoretical modeling suggested the presence of such intermediate reactive species such as and iodide adduct with ozone ($I{\cdot}OOO^-$) (Gálvez et al. 2016 and references therein) and demonstrated different reaction pathways for the hydrated and bare iodide with iodite (IO_2^-) being the predominant product for the hydrated iodide (Teiwes et al. 2019). This literature information suggests that oxidation of iodide with ozone in the tank waste environment is likely.

Overall, the aqueous chemistry of iodine is extremely complex and sensitive to the process conditions, including pH, solution composition, presence of redox constituents, iodine concentration, temperature, material of contact surface, and others. Over the past decades, extensive research has been specifically aimed at prediction and control of the formation of volatile radioactive iodine species and their atmospheric releases during reactor operation or off-normal events, and has significantly advanced the understanding of iodine behavior and generated relevant databases of thermodynamic and kinetic parameters of iodine reactions (Wren et al. 2000 and references therein).

These fundamental thermodynamic considerations regarding iodine behavior can guide prediction of its redox and chemical speciation in the absence of high radiation fields and therefore are applicable to the assessment of iodine behavior in the tank waste process streams post removal of Cs-137 by CST ion exchange. However, in presence of high radiation fields, iodine thermodynamic models are not suitable because generated water radiolysis products rapidly and continuously react with iodine species, preventing thermodynamic equilibrium from being reached. Progression of these reactions governs iodine behavior and eventually lead to the formation of products which are not only thermodynamically stable but also less suspectable to radiolytic conversions. These radiolysis-driven reactions are expected to occur in the Hanford tanks. However, the reactions are expected to be dissimilar to those described by the literature as those studies focus on iodine radiolytic behavior in nuclear fuel and related streams, which would be an acidic reactor environment, contrary to alkaline Hanford wastes. Only sporadic studies of iodine radiolysis in basic solutions are available, and these are discussed in Section 3.3.

3.2 Solubility of Iodide/Iodate

Iodide forms highly insoluble compounds with Ag(I), Bi(III), Cu(I), Hg(I, II), Pb(II), and Tl(I); iodate forms low-solubility compounds with a wide range of alkaline earth, transition, and post-transition metal ions, which are generally more soluble than iodides (

Table 3.1). It should be noted that in concentrated solutions typical for Hanford supernatants, activity of water and ionic species is greatly reduced, and due to non-ideality effects the thermodynamic K_{sp} reported in

Table 3.1 will have greater effective values at high ionic strength. For instance, solubility of $CaSO_4$ (K_{sp} = 2.63×10^{-5}) increased from 0.016 in pure water to 0.023 in 0.25 M NaCl (Willey 2004). Similar increases of solubility with ionic strength were documented for PbI_2 (Clever and Johnston 1980). Correction of K_{sp} values for high-ionic-strength complex solutions is difficult because it requires knowledge of activity coefficients for the analytes of interest and availability of corresponding thermodynamic models, which are largely lacking.

Solubility of iodides can increase due to potential formation of high-order anionic complexes $M^{m+}I_i^{m-i}$ where i > m, which have a tendency to aggregate into colloidal species as was demonstrated for AgI (Lanford and Kiehl 1941) and PbI_2 (Lanford and Kiehl 1941; Clever and Johnston 1980), albeit they typically occur at elevated iodide concentrations. Mixed halide complexes $M^{m+}Cl_c I_i^{m-c-i}$ are also possible.

Table 3.1 suggests that transition and post-transition metal ions are easily hydrolyzed and form very insoluble hydroxide compounds; they are also expected to undergo further hydrolysis in the highly alkaline tank waste, generating anionic species with general composition $M^{m+}(OH)_n^{m-n}$ where n > m. For instance, X-ray absorption measurements suggested that $Pb(OH)_3^-$ species dominate in NaOH solutions ranging from 4 to 16 M (Bajnóczi et al. 2014); however, other studies identified higher-order Pb hydroxides and polynuclear species (Cruywagen and Van de Water 1993; Lothenbach et al. 1999). Bi forms a variety of hydroxide and oxyhydroxide species and is very susceptible to polymerization in alkaline solutions (Lothenbach et al. 1999). This implies that the CuI, PbI_2, TlI, and transition/post-transition metal iodate compounds outlined in

Table 3.1 are also susceptible to hydrolysis, increasing the solubility of iodide and iodate ions. Mixed hydroxo-halide colloidal complexes $M^{m+}(OH)_n I_i^{m-n-i}$ are deemed likely to be present in Hanford tank waste. Bi^{3+} readily forms oxoiodide compounds with variable compositions, which also can promote formation of the colloidal iodide species in Hanford tank waste. Measurements of Pb and Bi phases in Hanford tank wastes have been made previously (Herting et al. 2015, Reynolds et al. 2015). Notable exceptions are AgI, HgI_2, and alkaline earth iodates, which are expected to be relatively stable to hydrolysis. However, alkaline earth metal ions form very insoluble complexes with phosphate and sulfate, which undoubtedly will outcompete iodate and increase its solubility.

In summary, it is evident that Ag(I) and Hg(I, II) are expected to control aqueous solubility of iodide. A single phase potentially controlling solubility of iodate could be $Bi(IO_3)_3$; however, no quantitative information on its K_{sp} value was found in the literature.

Table 3.1. Solubility product constants for iodide and iodate inorganic salts. Taken from *CRC Handbook of Chemistry and Physics* (Haynes 2014)

Iodide Compound	K_{sp}	Iodate Compound	K_{sp}	Hydroxides	K_{sp}
AgI	8.52×10^{-17}	$AgIO_3$	3.17×10^{-8}	$Ba(OH)_2$	5×10^{-3}
BiI_3	7.71×10^{-19}	$Ba(IO_3)_2$	4.01×10^{-9}	BiOOH	4×10^{-10}
CuI	$1.2\ 7\times 10^{-12}$	$Ba(IO_3)_2 \cdot H_2O$	1.67×10^{-9}	$Ca(OH)_2$	5.02×10^{-6}
Hg_2I_2	5.2×10^{-29}	$Bi(IO_3)_3$	Insoluble[a]	$Cd(OH)_2$	7.2×10^{-15}
HgI_2	2.9×10^{-29}	$Ca(IO_3)_2$	6.47×10^{-6}	CuOH	2.0×10^{-15}
PbI_2	9.8×10^{-9}	$Ca(IO_3)_2 \cdot 6H_2O$	7.10×10^{-7}	$Cu(OH)_2$	1.1×10^{-15}
TlI	5.54×10^{-8}	$Cd(IO_3)_2$	2.5×10^{-8}	$Hg(OH)_2$	3.6×10^{-26}
--	--	$Cu(IO_3)_2 \cdot H_2O$	6.94×10^{-8}	$Mn(OH)_2$	2.0×10^{-13}
--	--	$La(IO_3)_3$	7.50×10^{-12}	$Ni(OH)_2$	5.48×10^{-16}
--	--	$Pb(IO_3)_2$	3.69×10^{-13}	$Pb(OH)_2$	1.43×10^{-20}
--	--	$Mn(IO_3)_2$	4.37×10^{-7}	$Sr(OH)_2$	1.5×10^{-4}
--	--	$Ni(IO_3)_2$	4.71×10^{-5}	$Y(OH)_3$	1.00×10^{-22}
--	--	$Ra(IO_3)_2$	1.16×10^{-9}	$Zn(OH)_2$	3×10^{-17}
--	--	$Sr(IO_3)_2$	1.14×10^{-7}	--	--
--	--	$Sr(IO_3)_2 \cdot H_2O$	3.77×10^{-7}	--	--
--	--	$Sr(IO_3)_2 \cdot 6H_2O$	4.55×10^{-7}	--	--
--	--	$TlIO_3$	5.54×10^{-8}	--	--
--	--	$Y(IO_3)_3$	1.12×10^{-10}	--	--
--	--	$Zn(IO_3)_2 \cdot H_2O$	4.1×10^{-6}	--	--

(a) Schweitzer GK and LL Pesterfield. 2010. *The Aqueous Chemistry of the Elements*. Oxford University Press, USA.

3.3 Radiolysis of Iodine

Within the Hanford tanks, a strong irradiation environment exists and can directly influence the chemical behavior of species present, including iodine. Reactive species formed during radiolysis of water and NO_3^- have a strong influence on the aqueous speciation of iodine. Gamma radiation initiates a cascade of iodine redox reactions, including 1) oxidation of iodide leading to formation of intermediate HIO and volatile I_2 species (which also serves as a precursor to organo-iodine), and 2) reduction of iodate. The mechanisms of iodide oxidation and formation of organo-iodine (to a lesser extent) have been extensively studied in relationship to severe accidents at nuclear power plants ranging from very acidic pH to moderately alkaline (11 or 12). The following steps briefly summarize the iodide transformation in the presence of high radiation fields (Wren 2005; Kim et al. 2018).

1. Radiolysis-induced oxidation of iodide to form molecular iodine I_2, which partitions between aqueous and gaseous phases.
2. In the aqueous phase, I_2 can undergo the following processes:
    a. Radiolytic reduction back to iodide,
    b. Further oxidation first to HIO/IO^- and then to non-volatile iodine oxides such as iodate,
    c. Hydrolysis and disproportionation to iodide and iodate,
    d. I_2 and transient iodine species can react with organic compounds to form organic iodides.

These processes are schematically depicted in Figure 3.3.

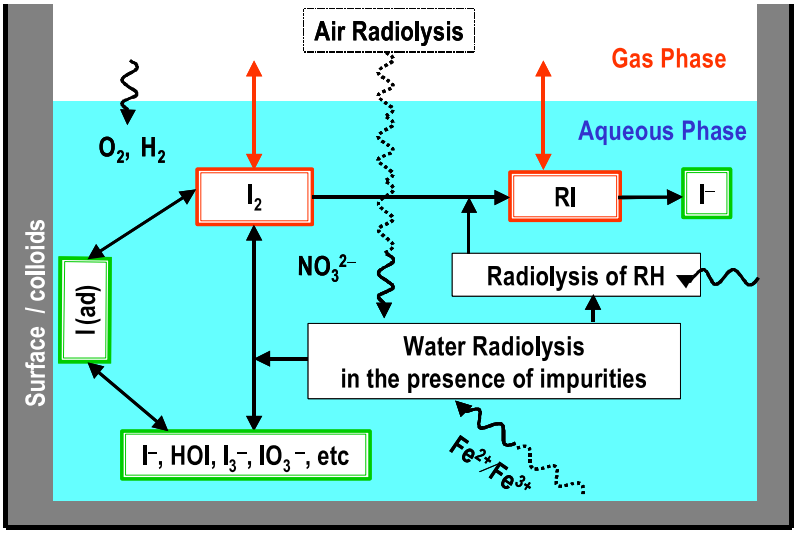

Figure 3.3. Schematic of iodide radiolytic transformations in aqueous solutions. Adapted from Wren (2005).

The reaction pathways are highly pH-dependent, and in alkaline solutions the hydrolysis-driven decomposition of I_2 was shown to dominate, thereby suppressing its volatilization (Truesdale et al. 1994). Lin and Chao (2009) summarized iodide radiolytic reactions, and in the alkaline solutions they can be represented by Eqs. (3.4) through (3.9):

$$I^- + OH \rightarrow I + OH^- \quad (3.4)$$

$$I + OH \rightarrow HIO \quad (3.5)$$

$$I + I \rightarrow I_2 \quad (3.6)$$

$$I^- + HIO + H^+ \rightarrow I_2 + H_2O \quad (3.7)$$

$$I_2 + H_2O \rightarrow H^+ + I^- + HIO \quad (3.8)$$

$$HIO + nOH \text{ (successive oxidation)} \rightarrow IO_3^- \quad (3.9)$$

In Lin (1980), this mechanism was derived based on variable dose Co-60 irradiation of iodide solutions while systematically varying pH from 0 to 12, iodide concentration, and blanket gas (air or He) followed by spectroscopic analysis to identify resulting iodine species. The author showed that the yield of volatile I_2 was above 90% in highly acidic solutions and dropped precipitously starting at pH 3 to negligible at pH 7 and above. On the other hand, the yield of iodate generated by irradiation of iodide increased with the irradiation dose and was highly dependent on the initial iodide concentration and pH. Iodate was a predominant product at or below initial 10^{-6} M I^- at pH < 10 but formed only in very small quantities at 10^{-4} M iodide or above in the entire studied pH range. Solutions with 10^{-5} M iodide demonstrated intermediate regimes with iodate being a major product in a narrow pH range between about 7 and 10. The presence of 5×10^{-5} M Cu^{2+} added as free radical scavenger to the iodide solution at pH 7 retarded radiolytic formation of iodate at 10^{-4} M iodide but its effect was insignificant at 10^{-5} M total iodine.

In summary, Lin (1980) concluded that radiolytic oxidation of iodide to iodate was favorable in dilute iodine solutions at high radiation doses but suppressed at high pH. Additionally, in basic solutions, radiolytic oxidation of iodide generated only small quantities of I_2; this was attributed to its fast hydrolysis and formation of IO^-. Interestingly, these results are consistent with a study of volatile iodine formation in highly irradiated CsI solutions; the developed model accurately predicted experimental quantities of I_2 generated for 10^{-4} and 10^{-3} M iodine solutions but failed when iodine concentration was 10^{-5} M due to high concentrations of iodate produced (Nguyen et al. 2019). The reported conclusions should be accepted with caution because only a limited number of measurements were performed at elevated initial pH, and the final post-irradiation pH, which is expected to change in non-buffered irradiated solutions, was not recorded.

In the other review, Wren et al. (2000) noted that radiation-induced oxidation of iodide to I_2 is due to its reaction with the •OH radical occurring at very high rate. On the other hand, accumulation of I_2 in solution is primarily determined by three processes, including its hydrolysis and its reactions with H_2O_2 and superoxide anion O_2^- formed during water radiolysis. The hydrolysis of I_2 can be described by Eq. (3.10) at near-neutral pH and Eqs. (3.1) and (3.11) in alkaline solutions.

$$I_2 + H_2O \rightarrow I^- + HIO + H^+ \quad (3.10)$$

$$I_2 + OH^- \rightarrow I_2OH^- \quad (3.11)$$

Hydrogen peroxide is the primary water radiolysis product existing in an irradiated solution at a steady-state concentration (significantly higher than that of other radiolysis products) and plays an essential role in radiolytic transformations of iodine. It initiates multiple reactions, and Eqs. (3.12) through (3.15) correspond to the representative processes most applicable to alkaline conditions.

$$I_2 + H_2O_2 + 2H_2O \rightarrow 2I^- + O_2 + 2H_3O^+ \quad (3.12)$$

$$OI^- + H_2O_2 \rightarrow I^- + O_2 + H_2O \quad (3.13)$$

$$I_2OH^- + H_2O_2 \rightarrow IO_2H + I^- + H_2O \quad (3.14)$$

$$IO_2H + OH^- \rightarrow I^- + O_2 + H_2O \quad (3.15)$$

Inconsistencies were found in the literature regarding rate of I_2 oxidation by H_2O_2, which was explained by the variable catalytic effect of the solution buffers and media on iodine redox reactions (Schwarz and Bielski 1986; Bichsel and Von Gunten 2000). It should be noted that reaction of I_2 with H_2O_2 is relevant not only for the water radiolysis in the tanks, but also to the waste streams at ETF where H_2O_2 is utilized to aid organic destruction.

The superoxide anion O_2^- is a strong reductant and was noted as one of the water radiolysis products having major impact on radiolytic oxidation of iodide. Schwarz and Bielski (1986) concluded that O_2^- can react with I_2 via several pathways and identified formation of the I_2^- intermediate as a rate-controlling process that was found to be dependent on iodide concentration in the system and pH. In air-saturated solutions, generation of I_2^- peaked at 10^{-4} M iodide at near-neutral pH and was significantly reduced for more-dilute iodide solutions at lower or higher pH.

Previously it was demonstrated that the radiolytic transformation of iodine in the presence of nitrogen species is very complex; a set containing 47 entries of reactions and corresponding rate constants to simulate the radiolysis of I^- in N_2O^--saturated aqueous alkaline solutions was described (Buxton and Sellers 1985, Buxton and Mulazzani 2007). It was demonstrated that radiolytic oxidation of iodide at total

iodine concentration in the system at or below 10^{-5} M generates iodate as the predominant product under alkaline conditions and I_2 at pH less than 7. However, radiolytic oxidation of iodide to iodate requires the presence of oxygen, and in deaerated solutions, the fraction of generated iodate was greatly reduced. Cripps et al. (2011) compared formation of I_2 upon irradiation of iodide solution with or without the presence of NO_3^- at variable gamma dose and pH and found that nitrate significantly retards formation of I_2 even at high radiation doses. This retardation was enhanced in the air-saturated solutions in comparison with argon-sparged (Cripps et al. 2011).

Radiolysis of iodate is studied much less extensively than radiolysis of iodide; however, common trends are found in the literature. It is generally accepted that radiolysis of iodate generates iodine in unusual oxidation states of +4 and +6, as well as +7 and possibly +8, with various possible chemical identities as evident from optical spectroscopy (Klaning et al. 1981; Buxton and Sellers 1985; Mezyk and Elliot 1994). The reduction of iodine in high oxidation states (+6 and +7) back to iodate is fast, while I(+4) can be reduced to iodide or oxidized back to iodate. Limited experiments by Lin (1980) demonstrated that irradiation of 10^{-4} and 10^{-5} M iodate solution at pH 7 resulted in about a 40% reduction to iodide. However, iodate remained intact when its initial concentration was 10^{-5} M iodate under otherwise identical conditions. Increasing the pH to 10 facilitated nearly complete reduction to iodide (Mezyk and Elliot 1994).

Overall, it is evident that radiolysis is a key factor influencing iodine speciation in tank waste solutions. Prediction of radiation-induced iodine transformation in Hanford tank waste is difficult because of its complex composition of both inorganic and organic constituents, high radiation fields, and the multifaceted chemistry of iodine; however, based on the literature considerations discussed above, the most likely inorganic species are iodide, iodate, and organo-iodine. The formation of elemental iodine is significantly suppressed by its hydrolysis at alkaline pH in favor of IO^- and related intermediates, which are likely to promote transformation of iodide to iodate and possibly organo-iodine species in tank wastes. The organo-iodine role in radiolysis, and the limitations in available data, are discussed in Section 3.4.

The radiolytic transformation of iodide to iodate is facilitated by the following factors:

- Low concentration of total iodine (on the order of 10^{-5} M and below)
- Oxygen saturation
- Presence of nitrate
- Alkaline conditions

The presence of transition metal ions and organics with oxygen groups (e.g., alcohols and carboxylic acids), which are efficient scavengers of free radicals, hydrated electrons, and other reactive species formed during radiolysis, can modify radiolytic transformations of iodine. In addition, suppression of iodate formation at pH greater than 12 observed in dilute aqueous solutions may not be as pronounced or even occur in the highly concentrated brine-like media of the Hanford supernatants because of low activity of water and therefore greatly reduced effective pH while maintaining an oxygenated environment (Lin 1980). It should be noted that minimal work has been done to measure oxygen content of the Hanford wastes with one report observing oxygen in a tank AW-101 sample but without reasoning for its origin (Pederson and Bryan, 1996)

The behavior of iodine in tank waste chemistry is hard to predict from the information in literature. This technical gap can only be addressed through irradiation studies of Hanford tank waste or simulated tank waste environments.

3.4 Organo-Iodine in Tank Waste

The source of organo-iodine present in the wastes resulting from fuel dissolution is speculative; the organo-iodine is thought to arise from the interaction of I_2 with organic components such as grease, trace organics in acid or partitioning into the organic solvent phase during plutonium-uranium reduction-extraction in the Plutonium Uranium Extraction (PUREX) process (Burger 1991, Bruffey et al. 2015). It is also true that the iodine inventory has likely been in contact with other organic species, based on the history of waste transfer and mixing between tanks. A significant portion of the iodine is believed to be present in the complexant tanks; see Section 4.3. It is well known that organics influence technetium (Tc) speciation and result in the stability of non-pertechnetate forms of Tc in the tanks, specifically in the AN and SY tank farms (Chatterjee et al. 2018; Serne et al. 2014). Due to the strong correlation between the iodine and Tc inventories, Section 5.2, it is feasible that iodine speciation may be different within the complexant or high-organic containing tanks. Within the tanks with high organic content or identified as complexant tanks (e.g. AN-102, AN-107), the likelihood of organics partaking in the radiolysis processes is high and can further influence the iodine speciation. Many of the organics present in the waste can themselves undergo radiolysis to generate radical species which would react with species in the tank waste, including iodine. Ongoing work in fiscal year 2020[6] will give initial insight into this environment with speciation of a raw AN-102 sample, a tank which has measured a high fraction of non-pertechnetate Tc.

The yield of the organo-iodine products is thought to be highly dependent on the lifetime of the transient iodine species and the rates of their reactions with organics. No such information is available in the literature. It should be noted that because of high volatility of the CH_3I and abundance in the Hanford tank waste of various alkyl organic compounds with alcohol and carboxylate functionalities undergoing radiolysis, organo-iodine species other than CH_3I are expected to exist in the liquid tank waste fraction. It is also apparent that more than mono-substituted organo-iodine species (R-CH_2I, R-CHI_2, and R-CI_3) are possible, iodoform being a likely candidate. However, the speciation and distribution of organo-iodine in the Hanford tanks and resulting behavior through the flowsheet remains an unknown.

[6] October 1, 2019 through September 30, 2020.

4.0 Hanford Tank Farm Iodine Inventory

This section presents the technical basis for iodine speciation (total iodine, iodide, iodate, organo-iodine) in tank farms broadly as a function of waste phase, tank type, and final projected waste forms. During the Hanford fuel reprocessing era, 49.4 Ci of iodine-129 (I-129) were generated (Watrous and Wootan 1997). Of this total inventory, 4.7 Ci was discharged into liquid disposal sites and is now present in the subsurface. The BBI (on 5/18/2020) currently accounts for 28.41 Ci of I-129 in the tanks; see

Table 4.1. The remaining inventory is unaccounted-for and was either discharged to the atmosphere, captured by silver reactors during reprocessing, or released during tank leak events (Truex et al. 2017).

4.1 I-129 Inventory across Waste Phases

Due to the solubility of most iodine species and compounds, there is a clear split between where the iodine inventory partitions across the different waste phases in the tanks: supernatant, saltcake, and sludge.

Table 4.1 lists the total I-129 BBI content in each of the waste phases available from the Hanford Tank Waste Information Network System (TWINS). The supernatant (12.87 Ci) and saltcake (12.45 Ci total) contain the majority of the I-129, with a minor amount in the sludge (3.08 Ci total). Within BBI, the information with the most fidelity is that which comes from a direct sampling basis. A total of 11.17 Ci of I-129 can be attributed to sampling basis measurements, of which 9.46 Ci comes from supernatant samplings,

Table 4.1. A large portion of the projected supernatant inventory (12.87 Ci) can be accounted-for from sampling of the supernatant (9.46 Ci), while the other waste phases have less available sampling data. This places higher uncertainty on the iodine content of the other waste phases. Further sampling of the other waste phases should be performed to reduce this uncertainty, primarily the saltcake to determine how much of its iodine inventory will be immediately soluble during retrieval.

Table 4.1. Comparison of the I-129 inventory in the different waste phases based on the current BBI inventory available in TWINS. The total I-129 content is shown along with the portion of the I-129 that is accounted-for based on direct sampling data.

Waste Phase	I-129 Content (Ci)	I-129 Content with Sampling Basis (Ci)
All	28.41	11.17
Supernatant	12.87	9.46
Saltcake solid	8.00	0.55
Sludge (liquid and solid)	2.68	0.13
Saltcake (liquid and solid)	2.39	0.97
Saltcake interstitial liquid	2.06	0.07
Sludge solid	0.37	0.00
Sludge interstitial liquid	0.03	0.01

4.2 I-129 Inventory by Tank Type

The I-129 inventory splits based on all inventory bases between the DSTs (including the AN-, AP-, AW-, AY-, AZ- farms) and SSTs is presented in Table 4.2. The DSTs contain a larger inventory of I-129 at 16.76 Ci compared with 11.64 Ci in the SSTs. The DST inventory is primarily present in the supernatant (12.24 Ci), while the saltcake solid (7.58 Ci) contains the majority of the SST inventory since the majority of the waste fraction is in the saltcake form.

Table 4.2. Comparison of the I-129 inventory, using all sample bases, between the double-shell tanks and single-shell tanks.

Waste Phase	Double-Shell Tank I-129 Inventory (Ci)	Single-Shell Tank I-129 Inventory (Ci)
All	16.77	11.64
Supernatant	12.25	0.62
Saltcake solid	0.43	7.58
Sludge (liquid and solid)	1.81	0.87
Saltcake (liquid and solid)	1.81	0.58
Saltcake interstitial liquid	0.15	1.91
Sludge solid	0.29	0.07
Sludge interstitial liquid	0.03	0.00

4.3 I-129 Inventory in Farms Containing Complexant Tanks

Several tanks present in the AN- and SY- farms are considered as complexant tanks due to their high organic content and unique challenges, e.g. AN-102, AN-107, SY-101. One example of a challenge is the presence of complexants in a tank retaining more Sr-90 and transuranics in the supernatant phase (e.g., AN-102 and AN-107) compared to the sludge in which they would be expected to be found (Hallen et al. 2005; Peterson et al. 2018). Related to iodine speciation, the presence of complexants could facilitate higher concentrations of organo-iodine or other species, similar to how the complexant tanks show higher concentrations of non-pertechnetate species compared with the other tanks (Chatterjee et al. 2018; Serne et al. 2014). AN-farm (i.e., 7 DSTs) contains a large amount of I-129, close to 20% of the overall inventory at Hanford, with the largest inventory being present in tank AN-103 (1.205 Ci). SY-farm (i.e., 3 DSTs) holds 1.21 Ci of I-129. While many of the Hanford tanks contain high amounts of organics, the AN- and SY- tanks have high concentration of organic complexants in comparison with other tanks, and it is feasible that the inventory of I-129 in the AN- and SY- tanks may have a higher fraction of organo-iodine and different type of organo-iodine and behave differently in the Hanford flowsheet compared with iodide, iodate, or the organo-iodine in other tanks. The radiolysis pathways for the organic and complexant species would most likely be different in these tanks compared with the rest of the tank farms and common sense would dictate that differences in iodine speciation can arise as a result. Little is known about specific interactions/reactions that would occur and would be best identified through speciation measurements from these tanks.

Table 4.3. Comparison between the I-129 inventory, using all inventory bases, in the two tank farms containing complexant tanks, AN- and SY-farms.

Waste Phase	AN-Farm I-129 Inventory (Ci)	SY-Farm I-129 Inventory (Ci)
All	5.91	1.21
Supernatant	3.14	0.60
Sludge (liquid and solid)	1.37	0.08
Saltcake (liquid and solid)	1.25	0.53
Sludge solid	0.13	N/A
Saltcake solid	0.01	N/A
Saltcake interstitial liquid	0.01	N/A
Sludge interstitial liquid	0.004	N/A
N/A – Not applicable. Denotes a waste phase for which there is no available information in TWINS for that phase in the tank.		

4.4 Iodine-127 Inventory vs. Iodine-129

During fuel irradiation for reprocessing purposes, both I-129 and non-radiological I-127 are generated, with the amount of I-127 being ~20% to 25% of the amount of I-129 produced (Burger 1991). However, the data are sparse on the amount of I-127 in the Hanford waste tanks. The I-129 values in BBI, based on samples, were quantified using gamma emission analysis. I-127, being a stable isotope, would have no such signature and needs to be measured with mass spectroscopy. I-127 sampling data are available for only 9 of the 177 tanks (AN-104, AP-101, AW-101, AZ-101, BY-107, BY-108, C-104, S-102, and S-112). A recent report by Reynolds (2020) covers in detail the I-127 inventory. From this analysis, the fraction of I-127 compared with I-129 is variable. The I-127 inventory is higher than the I-129 inventory in all tank samples available except for AZ-101 and BY-107. Differences in iodine speciation are not expected to be related to the iodine isotope, but to the originating source of the iodine (Hou et al. 2009, 2013; Zhang et al. 2013), as discussed in Section 3.0.

The most recent flowsheet model runs only use the quantity of I-129. Some engineering applications may use the total iodine inventory and not just the I-129. An example would be a theoretical iodine capture/removal process at either the front or back end of the flowsheet that would need to account for total iodine in terms of media removal capacity and service lifetime. It should be noted that current model runs are based on experimental data with highly conservative amounts of iodine used in the testing.

5.0 Speciation in Tank Waste

Much of the current basis for iodine speciation in the Hanford tanks and in testing is based on the information summarized in a memo[7] with many assumptions made in place of data. This basis has directed how iodine species are treated in testing efforts related to the tanks, throughout the Hanford flowsheet and resulting waste form with iodide commonly viewed as the primary species. However, as discussed throughout this report, iodine speciation can influence the behavior iodine within the tanks and in specific unit operations. Thus, understanding the speciation of iodine originating in the tanks is required to most accurately project the routing of iodine through the flowsheet as the behavior in the melter and partitioning in the off-gas is influenced by the iodine species, as highlighted in recent work (Matlack et al 2020).

Based on the response of iodine in the various chemical conditions discussed in Section 3.0, it is likely that the assumed case for iodine speciation in the Hanford tanks in Section 5.1 does not represent the conditions within the tanks. To assess the validity of the iodine speciation assumptions, two approaches can be taken: 1) assessment of correlations between components and iodine within the known tank farm inventory, and 2) direct measurement of tank waste samples. Approach 1 is addressed in the subsections that follow. Approach 2 is being carried out – for the first time – this fiscal year by PNNL.

5.1 Prior Knowledge of Iodine Speciation at Hanford

Limited literature exists directly addressing the underlying technical arguments for iodine speciation in Hanford tank waste and any downstream effects of speciation throughout the Hanford flowsheet. The most detailed overview available is a meeting minutes memo from January 26, 2000, prepared by British Nuclear Fuels Limited (BNFL).[7] The memo provides expert opinions regarding iodine behavior in Hanford tank waste from two PNNL staff members (L. Burger and R. Scheele) and knowledge available at the time. Much of the information was based on an earlier iodine-related study (Burger 1991). Within this memo, the following understanding of iodine behavior was presented and to date remains the best summary resource for iodine behavior at Hanford.

All information in the following section (5.1.1) comes from the earlier reported information on iodine at Hanford and does not reflect the information presented throughout this report.

5.1.1 Iodine in Tank Waste Summarized by Burger 1991

Stable Species: The predominant liquid species at Hanford are iodide (I^-) and iodate (IO_3^-), likely associated with Na; both are stable in alkaline conditions. Organo-iodine (e.g., CH_3I) is much less prevalent. Some iodine may be present in solid phases as AgI or PdI_2. In the gas phase, the formation of iodine monochloride (ICl) is likely and the formation of nitrosyl chloride (NOCl) is a competitive reaction (Burger 1991). In the liquid phase, at high pH, HIO can form, but it is believed to exist primarily in solution and not in the gas phase (Burger 1991).

Iodide/Iodate Ratio: Based on the PUREX process chemistry, the iodide-to-iodate ratio is projected to be a fixed ratio of 9:1. This is larger than the simplistic case of adding iodine crystals to alkaline solutions, which would generate a 5:1 ratio. Going strictly from these assumptions and ignoring radiolysis products,

[7] BNFL. 2000. Meeting minutes from Iodine and Chemistry Process Discussion, Wednesday, January 26, 2000. No. 011233, British Nuclear Fuels Limited, Richland, Washington.

one would expect iodide to exceed iodate in the waste by > 5×. This ratio may be disturbed in high-organic or high-complexant tanks.

5.2 Chemical Marker Correlations

To support projections of iodine speciation within tank waste and liquid streams in the Hanford flowsheet, correlations between specific species/properties of the waste can be interrogated. These analyses can identify surrogates for soluble iodine, highlight potential interactions occurring with species in the waste, and assess the possibility of radiolysis influence and redox/pH conditions, which may drive speciation changes. Example markers, together with a brief justification for their consideration, are summarized below. It should be noted that the different separation processes executed at Hanford generated differing volumes of waste (Bi phosphate > REDOX > PUREX) and the concentration of radionuclides in these specific wastes would differ as a result. To compare resulting differences the species were evaluated using the values for the Inventory at Publication Date (total inventory) and Vector Concentrations (volume adjusted inventory).

1. **Tank supernatant redox potential:** As seen in Figure 3.1 and Figure 3.2, redox conditions heavily dictate iodine speciation. Direct measurement of supernatant redox potentials is possible, yet the authors could not find direct reports of the redox potentials. Corrosion potentials (E_{corr}) measured at the tank interface have been reported (directly in Tank AN-102) as being < -300 mV (vs. the saturated calomel electrode) for the supernatant and saltcake regions (Anda et al. 2009). This measurement would indicate a reducing environment. In place of a direct redox potential measurement, the NO_3^-/NO_2^- ratio is a suitable estimate of the redox potential; as the ratio gets larger, the supernatant would be more oxidizing and this ratio is used for corrosion control programs. This relationship could serve as a broad marker for the presence of any number of potential reductants for iodine (in oxidation states > -1, including I_2, IO^-, and iodate) that could facilitate reduction to iodide or interfere in radiolysis processes.
2. **Nitrite/Nitrate:** Nitrite and nitrate play critical roles in the corrosion behavior of the tanks and their ratio (along with hydroxide) defines corrosion control limits Nitrite is a known anodic inhibitor and helps prevent pitting corrosion and stress corrosion cracking initiation by shifting the corrosion potential of the steel anodically. Whereas nitrate can increase susceptibility to pitting corrosion. The ratio between the two can control these processes, and in turn, serve as a loose proxy for potential redox conditions within the tank. It is also known that electron capture by nitrate forms the strongly reducing electron-rich species like NO_3^{2-}, which in turn can act as reducing agents. This ratio cannot be used directly for estimation of E_h due to the myriad of other competing redox reactions, but is a viable comparison to make for iodine correlations.
3. **Cesium-137:** Within the supernatant, Cs-137 is a proxy to describe the energy available for reaction, as most of the other relatively abundant, high-energy nuclides (for example, ^{90}Sr, ^{60}Co, and ^{241}Am) are predominantly found in the sludge. Cs-137 can serve as an indicator of the total Hanford tank waste dose and energy available to generate reactive water and nitrate radiolysis species that 1) govern transformation of iodine species, and 2) lead to destruction of organic molecules and formation of reactive organic radicals, promoting formation of organo-iodine.
4. **Total organic carbon:** Assessment of the total organic carbon provides an indicator of a source of potential reactants to form organo-iodine and can be useful to predict iodine behavior during crystalline silicotitanate (CST) ion exchange; see Sections 7.4.2 and 7.4.3.

5. **Transition metals:** Assessment of transition metal content is beneficial to allow a potential proxy indicator for the presence of functionalized organic molecules, as these organics can react with transition metals and keep them soluble in the alkaline solutions. Functionalized organic molecules are more likely to be able to undergo radiolytic decomposition to form reactive organic radicals, which can comprise part of the total organic carbon measurement noted above. As well, many transition metals form low-solubility complexes with iodide and iodate, which can precipitate out but also can exist as colloids in Hanford tank waste, which potentially can be filtered out by CST.
6. **Hydroxide:** A measure of total alkalinity of the supernatant can serve as a broad indicator of 1) the extent of hydrolysis of transient iodine species formed in the course of radiolytic transformations, and 2) solubility of the potentially present colloidal iodide and iodate bound to the transition metals.
7. **Total Na:** The assessment of Na content can be used as a measure of the Hanford tank waste ionic strength and can serve as a marker of iodine solubility and behavior during tank waste operations such as retrieval, evaporator concentration, and others.

5.3 Correlation to Markers in Tank Waste

Correlations between iodine and key tank waste components were made using data downloaded (on 5/18/2020) from TWINS based on the current BBI. The TWINS data contain information on the compositions of various waste phases [all, supernatant, saltcake solid, saltcake interstitial liquid, sludge, saltcake (liquid + solid), and sludge (liquid+solid)], each with a different basis for the value [direct sampling (S), direct calculation (C), process knowledge (E), model-based template estimate (TE), and sample case template estimate (TS)]. The most reliable of these values are ones with a direct sampling basis (i.e., S). Two inventory sources were evaluated: 1) the Inventory at Publication Date, which represents the total inventory in a specific waste phase (units of Ci or kg), and 2) the Vector Concentration, which presents the concentration of the species relative to the mass of the specific waste phase (units Ci/g or kg/g). For the purpose of this report, two elements are reported as correlated when having an $R^2 > 0.60$. The plots of marker content vs. I-129 content used to assess the correlations are presented in Appendix A.

5.3.1 Inventory at Publication Date

A first correlation assessment was performed using the Inventory at Publication value (total units in the waste phase) using all available inventory basis types. A summary of the assessment of correlations between iodine and the species in each waste phase is presented in Table 5.1 using the R^2 value from a linear regression analysis as a surrogate for numerically representing the correlations. When combining all the data, the highest correlations are with Tc ($R^2 = 0.74$) and Na ($R^2 = 0.73$). This is not unexpected as the iodine content is tied to the amount of waste (Na) and other radionuclides (Tc) as much of the available data is based on estimates and associated correlations from other tanks. Within the supernatant, the correlations with Tc ($R^2 = 0.66$) and Na ($R^2 = 0.87$) remain but are also correlated with Al ($R^2 = 0.75$), Bi ($R^2 = 0.65$), and Cr ($R^2 = 0.63$). The Al and Bi are intriguing as they may be indicators of interactions with iodine due to the Al solubility and known complexation of iodine and Bi (

Table 3.1). Within the saltcake solid, the correlations are again with Tc ($R^2 = 0.82$) and Na ($R^2 = 0.82$) and also Ag ($R^2 = 0.75$) and Ba ($R^2 = 0.69$). Both Ag and Ba form insoluble compounds with iodide. Interestingly, the saltcake interstitial liquid has a correlation with Cs ($R^2 = 0.76$), Pb ($R^2 = 0.63$), Ag ($R^2 = 0.82$), Ba ($R^2 = 0.62$) and Hg ($R^2 = 0.80$) which might suggest an association between iodine and these elements that are known to precipitate low solubility phases (

Table 3.1). Only a small fraction of the iodine is expected in the sludge, Table 5.1, and any iodine present in the sludge most likely would be complexed with a metal cation or present in the interstitial liquid. It should be noted that with in BBI the "Sludge Solid" waste phase itself contains interstitial liquid, which is not independently separated from the "Sludge Interstitial Liquid" waste phase. This interstitial liquid component of the "Sludge Solid" may contain some of the iodine in that waste phase. The linear correlations observed in the sludge were with Ag ($R^2 = 0.91$), Ba ($R^2 = 0.99$) and Bi ($R^2 = 0.60$). Recently AgI was identified to be present on a sludge sample from tank C-105[8].

Table 5.1. List of the correlations, represented as linear regression R^2, between iodine and various tank waste components using *all inventory basis types and the Inventory at Publication Date value.*

All Data Types					
Phase Type:	All	Supernatant	Saltcake - Solid	Saltcake - Interstitial Liquid	Sludge
Element	R^2	R^2	R^2	R^2	R^2
Cs	0.45	0.27	0.46	0.76	0.34
Sr	0.03	0.06	0.03	0.02	0.13
Tc	0.74	0.66	0.82	0.86	0.41
Ag	0.04	0.39	0.75	0.82	0.91
Al	0.24	0.75	0.31	0.81	0.35
Ba	0.05	0.20	0.69	0.62	0.99
Bi	0.02	0.65	0.08	0.43	0.60
Cr	0.05	0.63	0.31	0.14	0.05
Fe	0.04	0.04	0.02	0.22	0.35
Free OH	0.59	0.57	0.33	0.75	0.00
Hg	0.01	0.03	0.11	0.80	0.23
Na	0.73	0.87	0.82	0.87	0.44
Pb	0.08	0.16	0.14	0.63	0.43
Total Organic Carbon	0.23	0.16	0.27	0.24	0.40
NO_3/NO_2 Ratio	0.03	0.01	0.07	0.24	0.10

However, much of the data included in TWINS is estimated (TE, TS, C, and E), and the sampling data (S) are the most indicative of the actual conditions in the tanks. The correlations between iodine and specific components were not as strong when only analyzing the sampling basis data, as shown in Table 5.2. Table 5.2 is the same analysis as Table 5.1, however only sampling data (S) from BBI was included. This result is also not unexpected, as the other four basis types use projected correlations to determine inventories (e.g., rad content). A finding of note is that fewer than four sampling points with iodine data were available for the saltcake and sludge, which does not allow correlations to be assessed on the sampling data for these waste phases. Within all the sampling data, the only correlation present was for Na ($R^2 = 0.67$). However, the correlations were heavily driven by the sampling data for tank AZ-101 which has a high content of Cs (4510000 Ci) and Tc (1280 Ci). Removing the data for AZ-101 from the dataset leads to correlations being measured for both Cs and Tc. For the supernatant sampling data, only Na had a linear correlation ($R^2 = 0.72$). Once again, the supernatant correlation was driven by AZ-101 and R^2 would be vastly improved for both Cs and Tc when removing AZ-101.

[8] Reynolds JG, JS Lachut, HK Meznarich, TM Ely, AM Templeton, GA Cooke. 2020 "Silver-iodide association in Hanford nuclear wastes" *Submitted to Journal of Radioanalytical and Nuclear Chemistry*. Release #WRPS-64599

Table 5.2. List of the correlations, represented as linear regression R^2, between iodine and various tank waste components using *only sampling basis data and the Inventory at Publication Date values.*

	Sampling Data (S)				
Phase Type:	All	Supernatant	Saltcake - Solid	Saltcake - Interstitial Liquid	Sludge
Element	R^2	R^2	R^2	R^2	R^2
[(a)]Cs	0.18	0.02	Only 4 iodine measurements	Only 2 iodine measurements	Only 3 iodine measurements
Sr	0.00	0.01	--	--	--
[(b)]Tc	0.48	0.29	--	--	--
Ag	0.00	0.11	--	--	--
Al	0.39	0.44	--	--	--
Ba	0.07	0.06	--	--	--
Bi	0.02	0.20	--	--	--
Cr	0.02	0.34	--	--	--
Fe	0.00	0.04	--	--	--
Free OH	0.25	0.21	--	--	--
Hg	0.00	0.00	--	--	--
Na	0.67	0.72	--	--	--
Pb	0.05	0.01	--	--	--
Total Organic Carbon	0.10	0.02	--	--	--
NO_3/NO_2 Ratio	0.08	0.12	--	--	--

(a) The all phases correlation with Cs improves to 0.72 with tank AZ-101 removed from the dataset as AZ-101 has a high Cs content (4510000 Ci)
(b)The supernatant correlation with Tc improves to 0.64 with tank AZ-101 removed from the dataset as AZ-101 has a high Tc content (1280 Ci)

5.3.2 Vector Concentration

The difference of the Vector Concentration data compared with the Inventory at Publication Date shown in Section 5.3.1 is that it is corrected for the mass of the waste phase of interest, thus taking into account the varying waste volumes. When analyzing the Vector Concentration data, the values from tanks AN-101, AN-106, and AZ-101 were removed. These three tanks have much higher iodine concentrations than the other 174 tanks and artificially skewed the correlations being evaluated. Tanks AN-101 and AN-106 have their high iodine content driven by estimates of sludge composition based on C-farm data and may produce suspect values that should be sampled and analyzed directly. Tank AZ-101 has a high iodine content measured from a supernatant sampling. Due to the uniquely high inventory of iodine in these tanks, it is valuable to assess the correlations between iodine and other species without the influence of these clear outliers.

Table 5.3 presents a similar dataset evaluation as Table 5.1 using the Vector Concentration data and viewing all the waste phases and all BBI bases, Table 5.3. The correlations observed are with Tc (R^2 = 0.69) and Na (R^2 = 0.66), similar to the Inventory at Publication Date data. These correlations are higher in the supernatant for Tc (R^2 = 0.76) and Na (R^2 = 0.68) and improve for Cs (R^2 = 0.71). The elements showing correlations are similar for the saltcake phases, with Cs (R^2 = 0.66) and Tc (R^2 = 0.78), being correlated in the solid and Cs (R^2 = 0.75), Tc (R^2 = 0.90), Na (R^2 = 0.77) and Al (R^2 = 0.64) in the interstitial liquid. Within the sludge, correlations were again observed for Ag (R^2 = 0.83) and Ba (R^2 = 0.65).

Table 5.3. List of the correlations, represented as linear regression R^2, between iodine and various tank waste components using *all inventory basis types and the Vector Concentration values.*

All Data Types					
Phase Type:	All	Supernatant	Saltcake - Solid	Saltcake - Interstitial Liquid	Sludge
Element	R^2	R^2	R^2	R^2	R^2
Cs	0.46	0.71	0.66	0.75	0.02
Sr	0.00	0.04	0.08	0.01	0.03
Tc	0.69	0.76	0.78	0.90	0.04
Ag	0.01	0.29	0.11	0.50	0.83
Al	0.05	0.50	0.29	0.64	0.14
Ba	0.00	0.07	0.20	0.38	0.65
Bi	0.12	0.02	0.11	0.04	0.00
Cr	0.15	0.03	0.43	0.13	0.00
Fe	0.01	0.01	0.02	0.02	0.00
Free OH	0.38	0.18	0.40	0.60	0.03
Hg	0.00	0.03	0.02	0.26	0.23
Na	0.66	0.68	0.50	0.77	0.02
Pb	0.00	0.14	0.00	0.46	0.01
Total Organic Carbon	0.20	0.18	0.16	0.20	0.01
NO_3/NO_2 Ratio	0.10	0.03	0.04	0.44	0.13

When moving to the sampling data (S) only in the Vector Concentration dataset, Table 5.4, the Tc (R^2 = 0.68), Cs (R^2 = 0.60) and Na (R^2 = 0.64) correlations are once again present in the supernatant, just as they were in the full analysis, Table 5.3. Although the correlations are not as large in the sampling data compared with the full dataset.

Table 5.4. List of the correlations, represented as linear regression R^2, between iodine and various tank waste components using *only sampling basis data and the Vector Concentration values.*

Sampling Data (S)					
Phase Type:	All	Supernatant	Saltcake - Solid	Saltcake - Interstitial Liquid	Sludge
Element	R^2	R^2	R^2	R^2	R^2
Cs	0.51	0.60	Only 4 iodine measurements	Only 2 iodine measurements	Only 2 iodine measurements
Sr	0.02	0.00	--	--	--
Tc	0.37	0.68	--	--	--
Ag	0.03	0.26	--	--	--
Al	0.02	0.52	--	--	--
Ba	0.02	0.01	--	--	--
Bi	0.13	0.02	--	--	--
Cr	0.00	0.04	--	--	--
Fe	0.04	0.00	--	--	--
Free OH	0.08	0.23	--	--	--
Hg	0.02	0.00	--	--	--
Na	0.14	0.64	--	--	--
Pb	0.07	0.01	--	--	--
Total Organic Carbon	0.00	0.00	--	--	--
NO_3/NO_2 Ratio	0.13	0.36	--	--	--

5.4 Chemical Marker Correlations Summary

The correlations evaluated between iodine and the tank constituents can strengthen the understanding of iodine speciation in the tank waste and assist in identifying trends that can be used to determine the universality of measurements of iodine speciation across the Hanford tanks. Based on the correlation analyses (i.e., two elements with $R^2 > 0.60$) of the tank components, the most common iodine correlations are with Tc and Na in both the “Inventory at Publication Date” and “Vector Concentration” datasets when all inventory bases are included and with only the sampling data (S). This correlation of iodine with Tc and Na suggests a distribution of iodine in the tanks determined by overall waste content.

In the liquid phases, supernatant and saltcake liquid, Al was also observed to be correlated with iodine. The Al correlation may need further characterization if processes that allow higher Al concentration in solution impact the amount of iodine, or its speciation. Bi also has a correlation with I in the supernatant. Sampling from B and BX farms, holding the Bi-phosphate process waste, would allow further assessment of Bi possibly precipitating iodine species (e.g., iodate,

Table 3.1). Within the saltcake, correlations were observed with species known to form insoluble phases with iodine including Ag, Pb, and Ba. While not being handled during DFLAW correlations were observed in the sludge for Bi, Ag and Ba suggesting the ~3 Ci of iodine projected to be in the sludge is associated with one of these cations as was recently shown in analysis of a C-105 sample,

Table 4.1. Thus, it is important to characterize the iodine fraction in the sludge as any iodine in the sludge is likely strongly bonded to a metal cation, which may impact speciation and recovery during eventual retrievals beyond the DFLAW timeframe.

6.0 Flowsheet Basis and Assumption

Despite uncertain iodine inventory and complex iodine speciation that varies with pH, radiolytic conditions, and chemical conditions, Hanford flowsheet modeling incorporates and tracks iodine (only as I-129) from the tank farms inventory, through waste processing operations, to final waste form disposition. Flowsheet modeling enables long-term planning while checking compliance with mass and concentration limits protecting facility designs and operating within permitting limits based on model assumptions derived on varying degrees of technical defensibility and integrity. To aid the assessment of flowsheet risk related to iodine speciation and inventory, a transparent accounting of the flowsheet modeling up through AP-106 is provided below based on current modeling assumptions.

6.1 Hanford Flowsheet Modeling of Iodine Speciation for Hanford Tank Waste

The primary flowsheet modeling objective for tracking I-129 inventory is for evaluation of secondary waste disposition. This is primarily through glass melt incorporation and adsorption on activated carbon absorbers in the LAW off-gas and vessel ventilation cleanup systems in both the WTP LAW and HLW facilities (Bernards et al. 2018). Key iodine tracking points also include 1) the liquid recycle stream [Effluent Management Facility (EMF) bottoms liquor] to WTP LAW, and 2) the 242-A evaporator and EMF evaporator overhead liquids transferring to the Liquid Effluent Retention Facility (LERF), followed by treatment in the ETF and final land disposal restriction (LDR) disposition in the IDF. However, the discussion here focuses specifically on I-129 inventory in Tank Farms and tracking up through AP-106. Nonetheless, the iodine inventory and speciation up through pretreatment (i.e., AP-106) directly impacts all subsequent flowsheet predictions and the associated I-129 risk in the aforementioned WTP LAW, EMF, and ETF facilities.

A simplified Tank Farms and pretreatment flowsheet illustrating iodine mass movements, phase changes, and stream splits is provided in Figure 6.1 to facilitate discussion. Although iodine has 37 known isotopes, only I-129 and I-127 are stable for any relevant timeframes (i.e., half-life greater than days). Furthermore, I-127 is a naturally abundant isotope with no regulatory restrictions. Therefore, the TOPSim model only tracks I-129 and this inventory mass enters the flowsheet model with no implied speciation (i.e., all I-129) and on a tank-by-tank basis tracked in the liquid or solid phase (Rasmussen 2019). During SST and DST solids retrievals, wash-leach factors (as specified in Pierson 2012) are applied, converting a fixed portion of the solid phase I-129 into the liquid phase. All 177 waste tanks have associated wash-leach factors for I-129 that vary from 0 (representing the case of no solid to liquid phase transfer of I-129) to 1 (a case where complete transfer of all solid phase I-129 to the liquid phase occurs). For example, a phase transfer of 58.2% or greater (i.e., 0.582 wash factor) for I-129, from the sludge or saltcake phase to the liquid phase, occurs in 26 DSTs and 130 SSTs, per the TOPSim model assumptions, during solids retrievals. Of this subset of SSTs and DSTs with wash factors of at least 58.2%, an assumed solid-to-liquid conversion of 100% is modeled for 100 SSTs and 5 DSTs, which highlights the high assumed solubility of iodine in the liquid phase. These retrieval assumptions significantly affect the I-129 inventory phase distribution within model space, may or may not be representative of reality, and have their underlying basis primarily documented (Hendrickson et al. 1998). The wash factors would be directly driven by the iodine speciation in the waste phase and the corresponding solubilities of the iodine compounds.

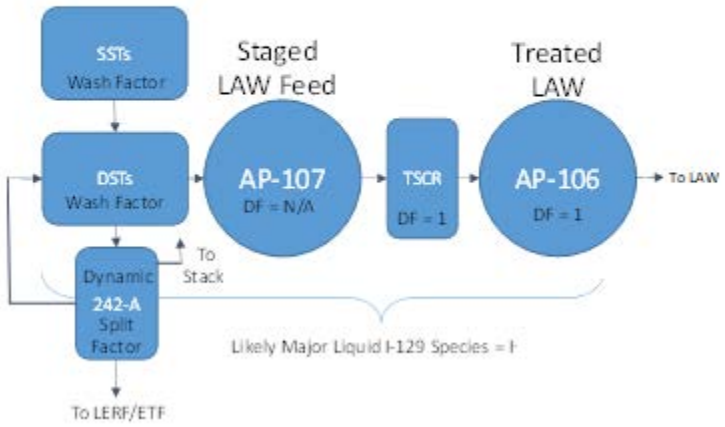

Figure 6.1. Simplified DFLAW flowsheet modeling of iodine for SST retrieval, DST staging, and pretreatment.

The liquid phase I-129 fraction is then either: a) stored in DSTs and fed forward into pretreatment facilities through a staged feed tank (currently AP-107), or b) evaporated in the 242-A evaporator. During evaporation in the 242-A evaporator, as specified by model equipment split factors[9] captured by Fleming and colleagues (2015), a portion of the I-129 is lost to the 242-A evaporator overheads, emitted out the stack or condensed, and transferred to LERF/ETF and disposed of per LDR regulations. The iodine model splits at the evaporator are dynamic while the condenser splits are static. These component splits for the 242-A evaporator are depicted in Figure 6.2 to aid the subsequent discussion.

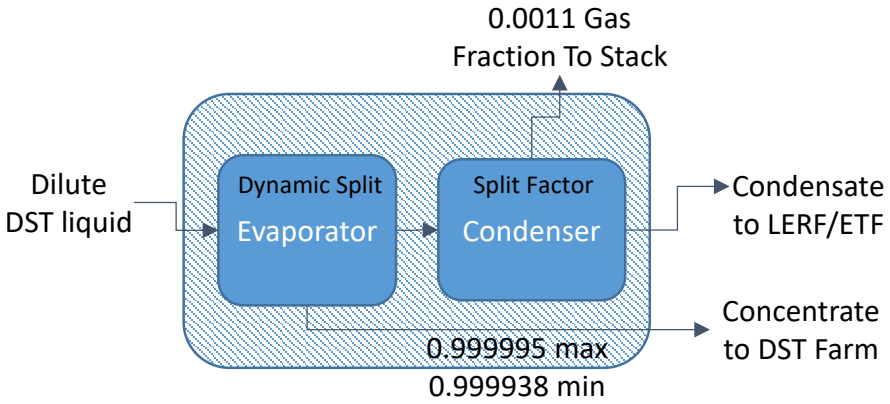

Figure 6.2. Simplified 242-A evaporator flowsheet modeling of iodine.

[9] Split factors can vary between 0 and 1 and represent a simple ratio of a specified destination stream (“TO”) divided by an inlet stream carrying the material into the operation (“FROM”); split factor = TO/FROM. These split factors are applied to all chemicals and radionuclides tracked by the model in the liquid, solid, and gas phases.

Any liquid or solid phase iodine entering the 242-A evaporator is modeled to volatilize initially to the vapor stream according to the split factor (SF_i) equation derived by Stamper (2012):

$$SF_i = \frac{1}{\left[1 + \frac{Kp_i}{18600}\left(\frac{1 - WVR}{WVR}\right)\right]} \quad (6.1)$$

where *WVR* (waste volume reduction) is the fractional waste volume reduction and the partition factor (Kp_i) for iodine is 4.00×10^8 as dictated by the associated calculation from WRPS.[10] Assuming a maximum fractional WVR of 0.57, as defined by Bernards et al. (2018) as the quotient of the maximum boil-off rate (i.e., 40 gpm) and the sum of the maximum boil-off rate and the minimum bottoms discharge rate (i.e., 30 gpm), the maximum predicted iodine evaporator split factor (SF_I) equals 6.16×10^{-5}, leading to a minimum fraction of iodine in the concentrate stream (0.999938). Assuming a minimum fractional WVR of 0.1, the minimum predicted iodine evaporator split factor equals 5.17×10^{-6}, leading to a maximum fraction of iodine in the concentrate stream (0.999995). In reality, the iodine (and component) split factor can vary per Eq. (6.1) as WVR values change depending on evaporator operating conditions; however, the dynamic evaporator split factor will decrease with decreasing WVR and the vast majority of the iodine remains in the evaporator concentrate (i.e., bottoms) as modeled. The vapor stream off the evaporator (i.e., overheads) passes through the demister/condenser unit, where the iodine partitioning is modelled by a fixed liquid and solid phase split factor of 0.0011, which represents a small fraction released to the 242-A stack and a majority remaining in the condensate for disposition to LERF/ETF.

In the next stage, the pretreatment processes of solids filtration and cesium removal by the TSCR system or the Low-Activity Waste Pretreatment System (LAWPS) are assumed to create no change in I-129 inventory or phase distribution within the flowsheet model. At this point in the flowsheet, treated Hanford tank waste feed has been generated by the TOC and is ready to be delivered in feed batches to BNI's WTP LAW Facility. As a reference to Tank Farms pretreatment discussion, during receipt, preparation, and staging of the melter feed in the WTP LAW Facility, no I-129 inventory or phase distribution changes are modeled within the flowsheet.

As the flowsheet model discussion highlights, the fate of iodine is highly dependent on liquid, solid, and gas phase iodine speciation as dictated by the chemical and thermal conditions of the various waste processing unit operations. These partitions and iodine species remain largely unverified by analyses of samples from representative processes using actual Hanford tank waste. However, in fiscal year 2020, PNNL is currently funded and performing inorganic iodine speciation of tank waste feed samples (i.e., AP-105, AP-107, and AN-102), AP-105 pretreatment effluents (i.e., post filtration and ion exchange), and melter off-gas condensate samples from the vitrification of pretreated AP-107 waste through the Radioactive Test Platform (RTP) continuous laboratory-scale melter. The work seeks to demonstrate I-129 speciation for initial DFLAW staged feed tanks as well as representative partitioning bases from opportunistic waste effluents derived from PNNL's RTP lab-scale waste processing unit operations (i.e., filtration, ion exchange, and melter). The work will establish defensible technical bases for iodine speciation and movements, from staged feed to melter off-gas condensate[11], to update flowsheet model assumptions and facilitate the development of an iodine abatement strategy, as needed.

[10] Calculation file titled "HTWOS Equipment Splits Rev 8.xlsx" (Eslin 2015). Spreadsheet verification document SVF-1778, Rev. 08.

[11] PNNL's Radioactive Test Platform lab-scale melter does not have a scaled prototypic off-gas system and the total melter off-gas condensate is collected as a composite, sampled, and iodine speciation measurements are assumed representative of full-scale, but no partitioning information is obtained.

7.0 Impact of Retrieval and Pretreatment on Iodine Speciation

7.1 Retrieval and Dilution

Based on the findings presented in the preceding sections, it is unlikely that iodine speciation will change during dilution and retrievals, as both the primary forms expected to be present, iodide and iodate, are stable in the waste environment. It should be noted that there is evidence that iodine concentration may dictate speciation resulting from radiolysis, although it is unknown if this process would occur in Hanford wastes and in the short time frames in which a waste phase is being retrieved.

However, the speciation in each waste phase must be known in order to allow predictions of recovery during retrievals. Retrieval of the supernatant should not be impacted by speciation, although in retrieval of the saltcake and sludge, the speciation of iodine and its associated cation will dictate at what rate the iodine is recovered.

In the saltcake, a correlation was observed with iodine and both Cs and Pb. This could indicate that these species could be associated with iodine and subsequently dictate the solubility; however, no corroborating experimental evidence currently exists. For the sludge, where no correlations were observed, iodine has been measured in sampling of the C-farm sludge. Knowing the associated phase and speciation of the iodine would allow an accurate assumption of the iodine recovery during sludge retrievals.

7.2 Theoretical Pretreatment Iodine Removal

If the removal of iodine from Hanford wastes (e.g. treated LAW, liquid secondary wastes) is to be targeted to improve waste management strategies[12] the speciation of iodine in the waste stream must be known. Iodine species directly influence many sorbents' capabilities to extract iodine, as most commercial sorbents will preferentially sequester iodide from solution compared with iodate and organo-iodine.

7.3 Evaporation

During evaporation (at the 242-A evaporator or within the EMF), testing suggests that iodine will remain in the concentrate in its iodide or iodate forms (Taylor-Pashow et al. 2019), especially with alkaline waste streams (Matlack et al. 2019). Neither of these recent efforts evaluated methyl-iodide or other organo-iodine species. Methyl iodide can decompose above 200 °C with an appropriate catalyst present (Nenoff et al. 2014). Evaporator testing of other volatile organics (e.g. acetonitrile, methylene chloride) in EMF evaporator conditions measured high partitioning to the condensate (Matlack et al. 2019). Stamper (2012) screened twenty 242-A Evaporator campaigns spanning 1994 to 2010, to derive an average partition coefficient basis for I-129 (and other analytes of interest) using feed and process condensate samples from 8 campaigns. Only I-129 concentrations were measured and I-129 partitioning to the concentrate is modeled to be greater than 99.9938% in both 242-A and EMF. The behavior of organo-iodine species in evaporator conditions is unknown and experimental work to observe partitioning or decomposition of the

[12] Report is currently under review and not yet publicly available. Skeen, RS, CA Langton, DJ McCabe, CA Nash, RM Asmussen, SA Saslow, IL Pegg, AG Misko. 2020. Evaluation of Technologies for Enhancing Grout for Immobilizing Hanford Supplemental Low Activity Waste (SLAW). SRNL-STI-2020-00228. Savannah River National Laboratory, Aiken, South Carolina.

organics is needed to close the gap (it should be noted that organic portioning in the 242-A evaporator is under evaluation in FY20 by Savannah River National Laboratory).

7.4 Feed to TSCR

The correlations between iodine and other waste constituents were performed using the input file obtained from WRPS, titled “Monthly AP-107 to TSCR Feed Vector Crosstab CaseID 9157.xlsx,” which projects the monthly composition of the liquid Hanford tank waste that will be fed to TSCR. This input file was used to examine the time-dependent profile of iodine in the Hanford tank waste feed composited from different tanks and therefore provides information on the iodine inventory in the feed to the LAW melter over time. The literature overview presented in the previous sections suggests that iodine behavior is concentration- and radiolysis-dependent, and spikes in iodine concentration can potentially point at the variability of its speciation and behavior; however, if total iodine (I-129 + I-127) concentration is on the order of or below 10^{-5} M, little to no variation in the iodine speciation and behavior is expected based on the observed correlations of I-129 concentration with other waste constituents (see Section 3.0 of this report).

Examination of the time profile suggests that the highest I-129 concentration in the Hanford tank waste feed will be at the beginning of the campaign and will peak at nearly 9×10^{-6} M in years 2022-2023 (Figure 7.1). This is followed by the gradual drop of iodine concentration with the minimum values being around 2×10^{-6} M. While this concentration range is less than an order of magnitude, one must remember that iodine properties depend on the total iodine concentration, including stable isotope I-127 in addition to radioactive I-129. A recent report by Reynolds (2020) summarized information on the inventory of I-127, which is available for nine tanks only. It appears to be on par with or greater than (up to about 7 times) the I-129 concentration. This implies that the concentration of total iodine in the TSCR feed will be in the 10^{-5} M range, significantly higher than shown in Figure 7.1 for I-129 and corresponds to even greater concentrations of iodine in the tank supernatants. This concentration is in the range where radiolytic conversion of iodide to iodate was suggested to be highly dependent on the total iodine concentration in the system (see Section 3.0 of this report), and therefore a change in the iodine speciation could take place.

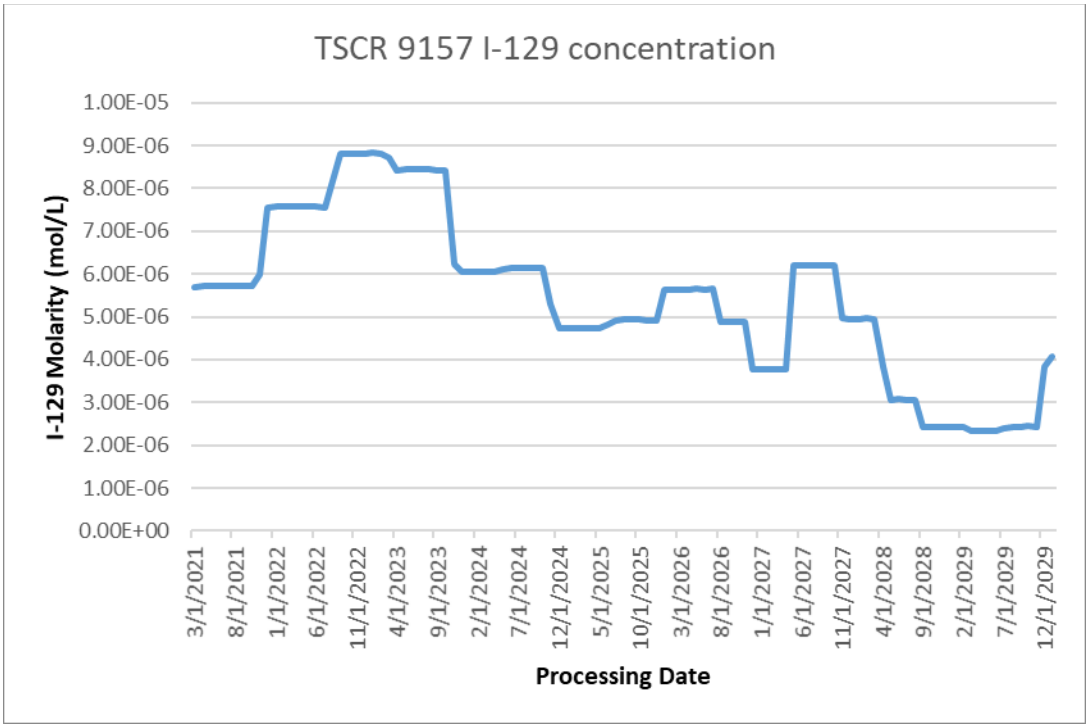

Figure 7.1. Concentration feed profile of I-129 throughout the lifetime of the DFLAW campaign.

7.4.1 Chemical Marker Correlations in Feed to TSCR

As for BBI analysis, the R^2 value from a linear regression analysis as a surrogate for representing the strength of a correlation of I-129 concentration with the TSCR feed constituents was adopted. In this evaluation, an R^2 value of above 0.6 was arbitrarily selected as being correlated just as in Section 5.2, and an R^2 between 0.3 and 0.6 is moderately correlating.

Table 7.1 summarizes correlation parameters for I-129 for the plots reported in Appendix B. It appears that some analytes, including Cs(133+137), Tc, Cl^-, NO_3^-/NO_2^-, and oxalate are correlated or moderately correlated with I-129 in the course of the entire campaign. It should be noted that correlation with Na is not possible since it is fixed at 5.6 M. Instead, highly soluble and relatively radiolysis-stable Cl^- can serve as a marker of the ionic strength, and therefore significant correlation is not surprising. Highly or moderately significant correlations with Cs, Tc, and NO_3^-/NO_2^- are consistent with those found in the raw supernatants based on the BBI analysis (Section 5.3). Significant and inverse correlation with oxalate is intriguing. The likely explanation is either the strong affinity of oxalate to the alkaline earth, transition, and post-transition metal ions, making them unavailable for coordination of iodide and iodate or the solubility of oxalate in TOPSim where lower Na equates to higher oxalate. It should be noted that the BBI influences the feed vector determination and some correlation may also be driven by solubility assumptions and not solely waste chemistry.

Other analytes, including total organic carbon, bound OH, Cu^{2+}, and Ni^{2+}, are correlated with I-129 concentration when input data for the 4/1/2037 to 7/1/2041 dates are separated into the individual subset. This subset is characterized by high total organic carbon content and therefore likely corresponds to the feed containing a significant fraction of the complexant wastes. These observations confirm conclusions drawn based on the BBI evaluation regarding dissimilar inventory, speciation, and behavior of iodine in the complexing waste. To this end, correlation with Cu^{2+} and Ni^{2+} is not surprising considering their properties as free-radical scavengers affecting radiolytic degradation of organics.

Few analytes exhibit moderate correlation with iodine, including Mo^{6+}, Be^{2+}, free OH^-, $Al(OH)_4^-$, and U(235+238). Correlation with aluminate is consistent with the findings for BBI. Interestingly, the majority of the transition and other metals that form insoluble compounds or complexes with I^- and IO_3^-, including Ag^+, Ba^{2+}, Bi^{3+}, Co^{3+}, Hg^+/Hg^{2+}, Pd^{2+}, Pb^{2+}, and Tl^{3+}, did not show any correlation with I-129 (data not shown).

Table 7.1. Evaluation of the correlations between iodine and the constituents on interest in the waste feed vectors in the feed to TSCR.

	Entire Campaign		Except 4/1/2037 - 7/1/2041		4/1/2037 - 7/1/2041	
	Slope	R^2	Slope	R^2	Slope	R^2
Highly or Moderately Correlated						
Cs(133+137)	7.4×10^{-2}	0.75				
Tc-99	1×10^{-1}	0.61				
Cl^-	8×10^{-5}	0.55				
NO_3^-/NO_2^-	-2×10^{-6}	0.46				
$C_2O_4^{2-}$	-4×10^{-4}	0.36				
TOC			3×10^{-5}	0.68	2×10^{-6}	0.97
Bound OH			9×10^{-4}	0.43	3×10^{-5}	0.84
Cu^{2+}			9×10^{-2}	0.28	1×10^{-2}	0.98
Ni^{2+}			9×10^{-3}	0.28	6×10^{-4}	0.99
Poorly Correlated						
Mo^{6+}	8×10^{-3}	0.26				
Be^{2+}	2×10^{-2}	0.21				
Free OH^-	2×10^{-6}	0.20				
$Al(OH)_4^-$	2×10^{-5}	0.19				
U(235+238)	-7×10^{-3}	0.18				

These results are in general agreement with the I-129 correlations for the tank supernatants generated based on the BBI inventory, not surprising as the TOPSIM feed is derived from BBI (Section 5.3).

7.4.2 TSCR – Post Filtration

Filtration of the TSCR feed using low-micron filters is not expected to change solution speciation of iodine and may only remove insoluble iodine species trapped in the solid particulates that are retained on the filter. Mercury-iodine compounds are likely candidates. Mercury speciation measurements on AP-107 feed and treated effluents from PNNL's RTP unit operations (i.e., post filtration and ion exchange) demonstrated 32% removal of feed mercury during filtration (Bottenus 2019). Removal of colloidal iodine likely present in the supernatant requires sub-micron filters, so colloidal iodine in the supernatant won't be affected.

7.4.3 TSCR – Post CST Ion Exchange

Processing of the filtered TSCR feed with CST ion exchange may result in the retention of some fractions of iodine on the CST in accord with the following considerations; however, targeted experimentation is needed to support these assumptions and quantify iodine retention by CST as a function of feed composition.

1. Retention of alkaline earth metal ions on the CST is well documented and has been demonstrated by test platform testing (Rovira et al. 2018). CST retains a significant fraction of Ca and removes Sr from the supernatants nearly quantitatively. As discussed in Section 3.2, iodate forms complexes with these metal ions and may be co-retained by the CST.

2. Iodide forms highly insoluble compounds with Hg and is likely to form colloidal species with Pb. Both Hg and Pb partition onto CST, and iodide can be co-retained. Bottenus (2019) conducted mercury speciation measurements on AP-107 feed and treated effluents from PNNL's RTP unit operations (i.e., post filtration and ion exchange) and demonstrated 20% removal of feed mercury during CST ion exchange.
3. Any other colloidal iodide/iodate and organo-iodine species can be filtered out by the CST.

8.0 Gaps and Conclusions

The information in this report represents a first-of-its-kind, thorough interrogation of the factors controlling iodine speciation in Hanford tank wastes, both in the tank and during its movement in the flowsheet through CST ion exchange. The following are the knowledge and technical gaps related to iodine speciation at Hanford.

From Section 3 (Chemical and Environmental Influences on Iodine Speciation):

Conclusion: The primary finding in the overview of the chemical and environmental factors is that radiolytic oxidation of iodide to iodate is undoubtedly occurring in the Hanford tank waste. Both iodide and iodate can be stable in alkaline environments at the projected pH (>12) yet their ratios will be dictated by the environment within the tanks. The original speciation of iodine generated during PUREX operations is predicted to be predominantly iodide and iodate in a 9:1 ratio (Burger 1991). Examination of the literature on radiolysis of iodine in alkaline solutions (albeit no reports covering conditions similar to the highly alkaline brine-like matrices of the tank waste supernatants are available) suggests radiolytic transformation of iodate. While the overall mechanism is complex, and the yield of iodate can be low, it is a continuous process that has occurred for several decades. The reverse reduction of IO_3^- to I^- is deemed to be much less efficient. Additionally, reductive stability of IO_3^- increases in alkaline solutions (Figure 3.2). Therefore, slow accumulation should take place and result in a steady increase of the iodate fraction, albeit quantitative prediction of the resulting iodide/iodate ratio is not possible without targeted radiolysis experiments using prototypical Hanford tank waste matrices, or without data from the ongoing fiscal year 2020 inorganic iodine speciation task.

As reviewed in the Section 3.0, radiolytic behavior of iodine is dependent on its solution concentration; in particular, nearly complete conversion of iodide to iodate is observed for the total iodine concentration in the system on the order or below 10^{-5} M. High nitrate concentrations and aerated conditions promote formation of iodate. Similar non-linear dependence of iodine behavior on its concentration can be anticipated in the LAW melter. Depending on the residence time in the melter plenum, thermodynamic equilibrium may not be reached and chemical transformation of the gaseous iodine species would depend on the kinetics of the associated processes and, therefore, on the concentration of the iodine in the gas phase, which is in turn a function of the iodine concentration in the Hanford tank waste feed.

Gaps: 1) There exists no thermodynamic foundation for understanding the iodine speciation and behavior for the conditions of the Hanford tank waste supernatants. Determination of the iodine E_h-pH diagram and iodine solubility in presence of alkaline earth ions, transition metal ions, and post-transition metal ions at extremely high ionic strength and alkalinity is needed. 2) The measurement and quantification of iodine species evolution and influence in Hanford waste environments under irradiation has not been pursued previously yet is crucial to projecting the universality of iodine speciation measurements across the tank farms. A matrix of iodide/iodate ratios in simulated tank waste can be irradiated and the changes in speciation ratios can be monitored to understand this technical gap. The presence of organics should be included in such an effort. Additionally, this should include assessment of iodine radiolysis at different concentrations and ratios of iodide/iodate. Further, it is recommended to conduct further opportunistic measures of inorganic iodine and organo-iodine species in raw tank waste samples received for use in PNNL's RTP to expand on those being performed in FY20.

From Section 4 (Tank Farm Inventory):

Conclusion: The evaluation of the distribution of the iodine inventory across the tank farms and the basis for that inventory highlighted some clear trends. The largest portion of the iodine inventory is projected to be present in the supernatant and saltcake solids (>70% total inventory). However, only the supernatant has a majority of its inventory documented by sampling events. The supernatant represents the primary phase associated with the known inventory within DSTs, whereas the primary phase associated with the known inventory within SSTs is the saltcake solids. Sampling and analysis of the other waste phases (non-supernatant) would improve confidence in the iodine inventory and assist in identifying speciation in those phases, which will be important during retrievals. There is a significant portion of the iodine inventory in the distributed evenly in the AN-farm, which contains complexant tanks. This is an important point, as the complexant tanks increase the likelihood of different organic associations of iodine and differing radiolysis effects on speciation.

Gap: The gap identified in the tank inventory analysis is the need for improved sampling to quantify the portion of the iodine not present in the supernatant, which then can be leveraged for identifying speciation within the other phases. The significant iodine fraction in the complexant or high-organic tanks highlights the need for better characterization of this inventory portion, primarily to identify the organo-iodine fraction, which may behave differently moving through the flowsheet and melter. Sampling all tanks is not feasible, but it is recommended that opportunistic measures of inorganic iodine, organo-iodine and other iodine isotopes (I-127) in raw tank waste samples received for use in PNNL's RTP or selected from 222-S archives be conducted.

From Section 5 (Speciation in Tank Waste):

Conclusion: In an overview of the current understanding of iodine speciation at Hanford, it appears that crucial factors such as radiolysis have been ignored. Correlations between iodine and chemical markers within the tank inventories were evaluated to determine conditions that may inform iodine speciation and behavior in the waste. No direct measurements of the tank redox potential were included in the assessment of the correlations between iodine and the other elements. When using sampling data, elemental correlations could only be developed for the supernatant due to a lack of data in the other phases. Based on the correlation analyses of the other tank constituents, linear correlations ($R^2 > 0.60$) between iodine and both Tc and Na were identified. In the liquid phases, supernatant and saltcake liquid, Al was also observed to be correlated with I. The Al correlation may be significant to characterize further if processes that allow higher Al concentration in solution influence the aqueous behavior of iodine. Bi has a correlation with I in the supernatant and sludge. Sampling from B and BX farms, holding the Bi-phosphate process waste, would allow further assessment of Bi possibly coordinating and/or precipitating iodine species (e.g., iodate). Correlations were observed, with minimal data points, in the sludge for Bi, Ag and Ba. Any iodine in the sludge is likely strongly bonded to a metal cation, which may impact speciation and recovery during retrievals, or may be dissolved in the interstitial liquid.

Gap: From the correlations, no trends were observed in the supernatant with elements that could precipitate iodine from the liquid phases, except for Bi. Correlations observed in the saltcake and sludge were observed with cations known to precipitate low solubility iodine phases and further characterization of the iodine in the saltcake and sludge is needed to assess these associations of iodine, which would dictate iodine recovery in retrievals. The iodine content is commonly correlated to Tc, meaning that there are many tanks with low inventories of both and would be opportunistic to target in a "sample and send" scenario with a parallel immobilization pathway; however, such an analysis of candidate tanks has yet to be formally documented.

From Section 6 (Flowsheet Basis and Assumption):

Conclusion: As the flowsheet model discussion in this section highlights, the fate of iodine is dependent on liquid, solid, and gas phase iodine speciation as dictated by the chemical and environmental conditions of the various waste processing unit operations. These partitions and iodine species remain largely unverified by analyses of samples from representative processes using actual Hanford tank waste. An example of this is the assumptions that led to wash factors used in TOPSim where the real-world response to retrieval conditions would be dictated by the solubility of the iodine compound in the saltcake or sludge.

Gap: Speciation of actual or simulated waste samples from representative unit operations continues to be a need to understand iodine behavior in the Hanford flowsheet. PNNL's RTP has provided opportunistic measures of inorganic iodine in raw tank waste samples as well representative effluents from laboratory-scale unit operations. Improved characterization of saltcake or sludge samples, either from 222-S archives or opportunistically from other tank waste sampling campaigns, to identify iodine species present would facilitate improved information fed to TOPSim.

From Section 7 (Impact of Retrieval and Pretreatment on Iodine Speciation):

Conclusion: The influence of iodine speciation and potential changes in speciation in the individual unit operations was evaluated. During retrievals, dilution will occur and is not likely to induce a speciation change during processing as dilution was only identified to influence radiolysis products over long periods. However, speciation in the parent phase needs to be known to determine wash factors for iodine. Knowing the speciation would contribute toward the selection of a iodine removal system or use of a getter in a cementitious waste form. During evaporation, iodide and iodate are projected to remain in the concentrate, while organo-iodine species may differ in partitioning. Similar chemical marker correlations as in the tank waste were identified in the feed to TSCR. Filtration will not impact iodine speciation and likely only retain insoluble iodine associated with solid particulate, like mercury. Upon entering the TSCR columns, iodine may be retained on CST due to the association of Hg, Pd, Ca, and Sr with the CST. The degree of interaction of the iodine and these species on CST will be dictated by the species of iodine present. Colloidal and organo-iodine have not been studied but may be filtered by the CST.

Gap: Once again the need to identify iodine speciation in the solid waste phases was highlighted, as it will dictate iodine behavior in retrievals. The interactions of iodine in TSCR should be evaluated using legacy samples or in future RTP feed and effluent samples to determine if any iodine is retained by the CST and if the amount retained is influenced by the presence of Pb, Hg, Ca, and Sr. These opportunistic measures of inorganic iodine and organo-iodine species in raw tank waste samples received for use in PNNL's RTP provide verified inventory inputs to the flowsheet model. Furthermore, measuring iodine partitioning using representative effluents from laboratory-scale unit operations would also address flowsheet modeling gaps related to presumptions of iodine behavior and mitigate iodine-related risks associated with the DFLAW mission phase.

9.0 References

Anda VS, GL Edgemon, AR Hagensen, KD Boomer, KG Carothers. 2009. *Corrosion monitoring in Hanford nuclear waste storage tanks, design and data from 241-AN-102 multi-probe corrosion monitoring system*. RPP-39917-FP. Washington River Protection Solutions, Richland, Washington.

ASME. 2000. *Quality Assurance Requirements for Nuclear Facility Applications*. NQA-1-2000, The American Society of Mechanical Engineers, New York, New York.

ASME. 2008. *Quality Assurance Requirements for Nuclear Facility Applications*. NQA-1-2008, The American Society of Mechanical Engineers, New York, New York.

ASME. 2009. *Addenda to ASME NQA-1-2008*. NQA-1a-2009, The American Society of Mechanical Engineers, New York, New York.

Bajnóczi ÉG, I Pálinkó, T Körtvélyesi, S Bálint, I Bakó, P Sipos, and I Persson. 2014. "Speciation and the structure of lead (II) in hyper-alkaline aqueous solution." *Dalton Transactions* 43(46):17539-17543.

Bates WF, TM Brouns, JR Cochran, AD Cozzi, GD Guthrie, RT Jubin, CA Langton, WG Ramsey, SM Robinson, N Soelberg, ME Stone, SD Unwin. 2019. *Report of Analysis of Approaches to Supplemental Treatment of Low Activity Waste at the Hanford Nuclear Reservation*. SRNL-RP-2018-00687. Savannah River National Laboratory, Aiken, South Carolina.

Beavers JA, N Sridhar, and KD Boomer. 2014. "Corrosion Management of the Hanford High-Level Nuclear Waste Tanks." *JOM* 66(3):491-502.

Bernards JK, TM Hohl, RT Jasper, N Pak, SD Reaksecker, AJ Schubick, LM Bergmann, AN Praga, and SN Tilanus. 2018. *TOPSim Model Requirements Document*. RPP-RPT-59470, Rev. 2A, Washington River Protection Solutions, LLC, Richland, Washington.

Bichsel Y and U Von Gunten. 1999. "Oxidation of iodide and hypoiodous acid in the disinfection of natural waters." *Environmental Science & Technology* 33(22):4040-4045.

Bichsel Y and U Von Gunten. 2000. "Hypoiodous acid: kinetics of the buffer-catalyzed disproportionation." *Water Research* 34(12):3197-3203.

Bottenus, C, MS Fountain, S Branch, G Gill and J Wood. 2019. *Mercury Speciation and Quantification of Hanford 241-AP-107 Tank Waste Feed and Treated Samples*. PNNL-29555, Rev.0. Pacific Northwest National Laboratory. Richland, Washington

Bruffey SH, BB Spencer, DM Strachan, RT Jubin, N Soelberg, BJ Riley. 2015. *A literature survey to identify potentially problematic volatile iodine bearing species present in off-gas streams.* ORNL-SPR-2015/290. Oak Ridge National Laboratory, Oak Ridge, Tennessee.

Bruffey SH, JA Jordan, RT Jubin, ML Parks, and TR Watkins. 2017. *Hot Isostatic Pressing of Engineered Forms of I-AgZ.* NTRD-MRWFD-2017-000412, Oak Ridge National Laboratory, Oak Ridge, Tennessee.

Burger LL. 1991. *Fission product iodine during early Hanford-Site operations: Its production and behavior during fuel processing, off-gas treatment and release to the atmosphere*. PNL-7210 HEDR, Pacific Northwest Laboratory, Richland, Washington.

Buxton GV and QG Mulazzani. 2007. "On the hydrolysis of iodine in alkaline solution: a radiation chemical study." *Radiation Physics and Chemistry* 76(6):932-940.

Buxton GV and RM Sellers. 1985. "Radiation-induced redox reactions of iodine species in aqueous solution. Formation and characterisation of I II, I IV, I VI and I VIII, the stability of hypoiodous acid and the chemistry of the interconversion of iodide and iodate." *Journal of the Chemical Society, Faraday Transactions 1: Physical Chemistry in Condensed Phases* 81(2):449-471.

Chatterjee S, VE Holfeltz, GB Hall, BM Rapko, SD Branch, AM Lines, SA Bryan, IE Johnson, WR Heineman, MS Fujimoto, and TG Levitskaia. 2018. *Characterization of Tc-99 Speciation and Chemical Composition of 241-AN-102 Tank Waste Supernatant*. PNNL-27730, Rev.0. Pacific Northwest National Laboratory, Richland, Washington.

Chia Y. 1958. "Chemistry of +1 Iodine in Alkaline Solutions." Ph.D. thesis. University of California, Berkeley, California.

Clever HL and FJ Johnston. 1980. "The solubility of some sparingly soluble lead salts: An evaluation of the solubility in water and aqueous electrolyte solution." *Journal of Physical and Chemical Reference Data* 9(3):751.

Cripps RC, B Jäckel, and S Güntay. 2011. "On the radiolysis of iodide, nitrate and nitrite ions in aqueous solution: An experimental and modelling study." *Nuclear Engineering and Design* 241:3333-3347.

Cruywagen J and R Van de Water. 1993. "The hydrolysis of lead (II). A potentiometric and enthalpimetric study." *Talanta* 40(7):1091-1095.

Deng Y, B Slettene, R Fundak, R Chen, M Gross, R Gimpel, and K Jun. 2016. *Flowsheet Bases, Assumptions and Requirements*. 25490-WTP-RPT-PT-02-005, Rev. 8, Bechtel National, Inc., Richland, Washington.

Doizi D. 2012. "Iodine Speciation in Nuclear Industry." DEN/DANS/DPC/SECR/LRMO, Saclay, France.

Fleming JT, JD Blesher, LJ Eslin, RT Jasper, RA Kirkbride, TD Woo, LM Bergmann, JK Bernards, SN Tilanus, and EB West. 2015. *Hanford Tank Waste Operations Simulator (HTWOS) Version 8.1 Model Design Document*. RPP-17152, Rev.12, Washington River Protection Solutions, LLC, Richland, Washington.

Gálvez Ó, M Teresa Baeza-Romero, M Sanz, and LF Pacios. 2016. "A theoretical study on the reaction of ozone with aqueous iodide." *Physical Chemistry Chemical Physics* 18(11):7651-7660.

Hallen RT, JG Geeting, MA Lilga, TR Hart, and FV Hoopes. 2005. "Assessment of the Mechanisms for Sr-90 and TRU Removal from Complexant-Containing Tank Wastes at Hanford." *Separation Science and Technology* 40(1-3):171-183.

Haynes WM (ed.). 2014. *CRC Handbook of Chemistry and Physics*. CRC Press.

Hendrickson DW, DE Place, GT MacLean, and SL Lambert. 1998. *Best-Basis Wash and Leach Factor Analysis*. HNF-3157, Rev. 0A, COGEMA Engineering, Richland, Washington.

Herting DL, GA Cooke, JS Page, and JL Valerio. 2015. *Hanford Tank Waste Particle Atlas*. LAB-RPT-15-00005, Rev.0. Washington River Protection Solutions, LLC, Richland, Washington.

Hou X, V Hansen, A Aldahan, G Possnert, OC Lind, and G Lujaniene. 2009. "A review on speciation of iodine-129 in the environmental and biological samples." *Analytica Chimica Acta* 632(2):181-196.

Hou X, PP Povinec, L Zhang, K Shi, D Biddulph, C-C Chang, Y Fan, R Golser, Y Hou, M Ješkovský, AJT Jull, Q Liu, M Luo, P Steier, and W Zhou. 2013. "Iodine-129 in Seawater Offshore Fukushima: Distribution, Inorganic Speciation, Sources, and Budget." *Environmental Science & Technology* 47(7):3091-3098.

Kim T, M Kim, S-H Jung, and J-W Yeon. 2018. "Volatility of radioactive iodine under gamma irradiation: effects of H_2O_2 and NaOH on the decomposition rate of volatile molecular iodine dissolved in aqueous solutions." *Journal of Radioanalytical and Nuclear Chemistry* 316(3):1267-1272.

Klaning U, K Shehested, and T Wolff. 1981. "Laser Flash Photolysis and Pulse Radiolysis of Iodate and Periodate in Aqueous Solution." *Journal of the Chemical Society Faraday Transactions* 77:1707-1718.

Lanford OE and SJ Kiehl. 1941. "The solubility of lead iodide in solutions of potassium iodide-complex lead iodide ions." *Journal of the American Chemical Society* 63(3):667-669.

Latimer WM. 1952. *Oxidation Potentials*. New York, New York, Prentice-Hall.

Lin C-C. 1980. "Chemical effects of gamma radiation on iodine in aqueous solutions." *Journal of Inorganic and Nuclear Chemistry* 42(8):1101-1107.

Lin C-C and J-H Chao. 2009. "Reassessment of reactor coolant and iodine chemistry under accident conditions." *Journal of Nuclear Science and Technology* 46(11):1023-1031.

Lothenbach B, M Ochs, H Wanner, and M Yui. 1999. *Thermodynamic data for the speciation and solubility of Pd, Pb, Sn, Sb, Nb and Bi in aqueous solution*. JNC-TN-8400-99-011, Japan Nuclear Cycle Development Institute, Tokyo, Japan.

Matlack KS, H Abramowitz, M Brandys, and IL Pegg. 2019. *EMF Evaporation Testing to Support WTP Start-Up and Flowsheet Development*. VSL-19R4640-1, Vitreous State Laboratory, The Catholic University of America, Washington, D.C.

Matlack KS, H Abramowitz, IS Muller, I Joseph, and IL Pegg. 2020. *Iodine Speciation Effects in LAW Feeds*. VSL-20R4740-1, Vitreous State Laboratory, The Catholic University of America, Washington, D.C.

Mezyk S and A Elliot. 1994. "Pulse Radiolysis of Iodate in Aqueous Solution." *Journal of the Chemical Society Faraday Transactions* 90(6):831-836.

Nenoff TM, MA Rodriguez, NR Soelberg, and KW Chapman. 2014. "Silver-mordenite for radiologic gas capture from complex streams: Dual catalytic CH3I decomposition and I confinement." *Microporous and Mesoporous Materials* 200:297-303.

Nguyen TTT, KS Ha, JH Song, and SI Kim. 2019. “An Estimation of Volatile Iodine in a Pool at Low pH and High Iodide Concentrations Under Irradiation.” *Nuclear Science and Engineering* 193(8):916-925.

Parry EP and DH Hern. 1973. “Stoichiometry of ozone-iodide reaction: Significance of iodate formation.” *Environmental Science & Technology* 7(1):65-66.

Pederson LR, SA Bryan. 1996. *Status and Integration of Studies of Gas Generation in Hanford Wastes*. PNNL-11297. Pacific Northwest National Laboratory, Richland, Washington.

Peterson RA, EC Buck, J Chun, RC Daniel, DL Herting, ES Ilton, GJ Lumetta, and SB Clark. 2018. “Review of the Scientific Understanding of Radioactive Waste at the U.S. DOE Hanford Site.” *Environmental Science & Technology* 52(2):381-396.

Pierson KL. 2012. *Double-Shell and Single-Shell Tank Inventory Input to the Hanford Tank Waste Operations Simulator Model – 2012 Update*. RPP-33715, Rev.5. Washington River Protection Solutions, LLC. Richland, Washington.

Prindville, KA. 2016. *Inventory Data Package for the Integrated Disposal Facility Performance Assessment*. RPP-ENV-58562, Rev. 3. Washington River Protection Solutions, LLC. Richland, Washington

Rasmussen J. 2019. *Guidelines for Updating the Best-Basis Inventory.* RPP-7625, Rev. 14, Washington River Protection Solutions, LLC, Richland, Washington.

Reynolds, JG, J S Page, GA Cooke, and JA Pestovich. 2015. “A Scanning Electron Microscopy Study of Bismuth and Phosphate Phases in Bismuth Phosphate Process Waste at Hanford”. *Journal of Radioanalytical and Nuclear Chemistry* 304, 1253-1259

Reynolds JG. 2020. "Uncertainty and Variability of Iodine in WTP DFLAW Feed". RPP-RPT-62615. Washington River Protection Solutions, LLC. Richland, Washington.

Rovira AM, SK Fiskum, HA Colburn, JR Allred, MR Smoot, and RA Peterson. 2018. *Cesium Ion Exchange Testing Using Crystalline Silicotitanate with Hanford Tank Waste 241-AP-107*. PNNL-27706, Pacific Northwest National Laboratory, Richland, Washington.

Schwarz HA and BH Bielski. 1986. “Reactions of hydroperoxo and superoxide with iodine and bromine and the iodide (I2-) and iodine atom reduction potentials.” *The Journal of Physical Chemistry* 90(7):1445-1448.

Serne RJ, BM Rapko and IL Pegg. 2014. *Technetium Inventory, Distribution, and Speciation in Hanford Tanks*. PNNL-23319 Rev.1; EMSP-RPT-022 Rev.1, Pacific Northwest National Laboratory, Richland, Washington.

Stamper LJ. 2012. *Recommendation for Updating Evaporator Partition Coefficients*. RPP-RPT-52097, Rev. 0, Washington River Protection Solutions, LLC, Richland, Washington.

Taylor-Pashow KML, AS Choi, DL McClane, and DJ McCabe. 2019. *Iodine Distribution During Evaporation of Hanford Waste Treatment Plant Direct Feed Low Activity Waste Effluent Management Facility Simulant*. SRNL-STI-2019-00471, Rev.0. Savannah River National Laboratory, Aiken, South Carolina.

Teiwes R, J Elm, M Bilde, and HB Pedersen. 2019. “The reaction of hydrated iodide I(H2O)− with ozone: a new route to IO2− products.” *Physical Chemistry Chemical Physics* 21(32):17546-17554.

Tranbarger R. 2018. *LAW Primary Offgas Process (LOP) and LAW Secondary Offgas/Vessel Vent (LVP) System Design Description*. 24590-LAW-3ZD-LOP-00001, Rev. 2, Bechtel National, Inc., Richland, Washington.

Truesdale V, C Canosa-Mas, and G Luther III. 1994. “Kinetics of Disproportionation of Hypoiodous Acid.” *Journal of the Chemical Society Faraday Transactions* 90(24):3639-3643.

Truex MJ, BD Lee, CD Johnson, N Qafoku, JE Szecsody, JE Kyle, MM Tfaily, M Snyder, KJ Cantrell, and DL Saunders, AJ Lawter, M Oostrom, GD Tartakovsky, IL Leavy, E McElroy, D Appriou, R Sahajpal, M Carroll, R Chu, EA Cordova, GV Last, MH Lee, DI Kaplan, WL Garcia, S Kerisit, O Qafoku, ME Bowden, FN Smith, J Toyoda and AE Plymale. 2017. " *Conceptual Model of Iodine Behavior in the Subsurface at the Hanford Site*. PNNL-24709, Rev. 2. Pacific Northwest National Laboratory, Richland, Washington.

USDOE. 2018. *Performance Assessment for the Integrated Disposal Facility, Hanford Site, Washington*. RPP-RPT-59958, Rev. 1, Washington River Protection Solutions, LLC, Richland, Washington.

Uytioco E. 2019. *Tank Farm Waste Transfer Compatibility Program*. HNF-SD-WM-OCD-015, Rev. 50. Washington River Protection Solutions, LLC, Richland, Washington.

Vienna JV. 2015. “Closed Fuel Cycle Waste Treatment Strategy” PNNL-24114. Pacific Northwest National Laboratory, Richland, Washington.

Watrous RA and DW Wootan. 1997. *Activity of Fuel Batches Processed Through Hanford Separations Plants 1944 Through 1989*. HNF-SD-WM-TI-794, CH2M Hill Hanford Group, Richland, Washington.

Willey JD. 2004. “The Effect of Ionic Strength on the Solubility of an Electrolyte.” *Journal of Chemical Education* 81(11):1644.

Wren JC. 2005. “Radioiodine chemistry: The unfinished story.” *Proceedings of the European Review Meeting on Severe Accident Research (ERMSAR) 2005*, November 14-16, 2005, Aix-en-Provence, France.

Wren JC, J Paquette, S Sunder, and BL Ford. 1986. “Iodine chemistry in the +1 oxidation state. II. A Raman and uv–visible spectroscopic study of the disproportionation of hypoiodite in basic solutions.” *Canadian Journal of Chemistry* 64(12):2284-2296.

Wren JC, JM Ball, and GA Glowa. 2000. “The chemistry of iodine in containment.” *Nuclear Technology* 129(3):297-325.

Zhang L and X Hou. 2013. “Speciation analysis of ^{129}I and its applications in environmental research.” *Radiochimica Acta* 101(8):525-540.

Zhang S, C Xu, D Creeley, Y-F Ho, H-P Li, R Grandbois, KA Schwehr, DI Kaplan, CM Yeager, D Wellman, and PH Santschi. 2013. “Iodine-129 and Iodine-127 Speciation in Groundwater at the Hanford Site, U.S.: Iodate Incorporation into Calcite.” *Environmental Science & Technology* 47(17):9635-9642.

Appendix A – Correlation Plots from Inventory at Publication Date

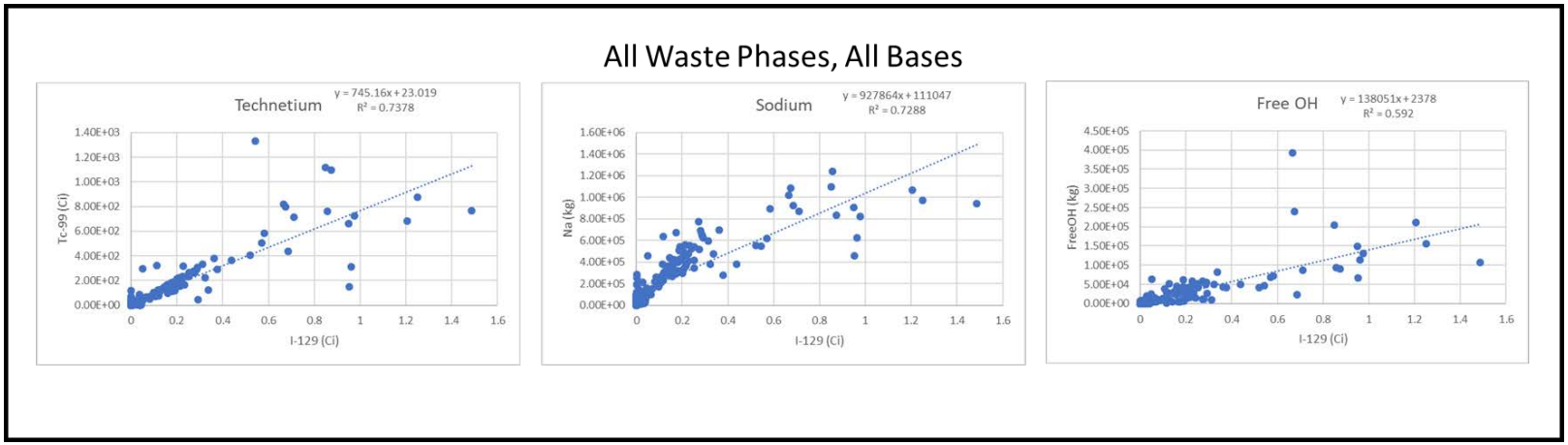

Figure A.1. Plots used to determine correlations between I-129 and specific elements using all waste phases and all inventory bases.

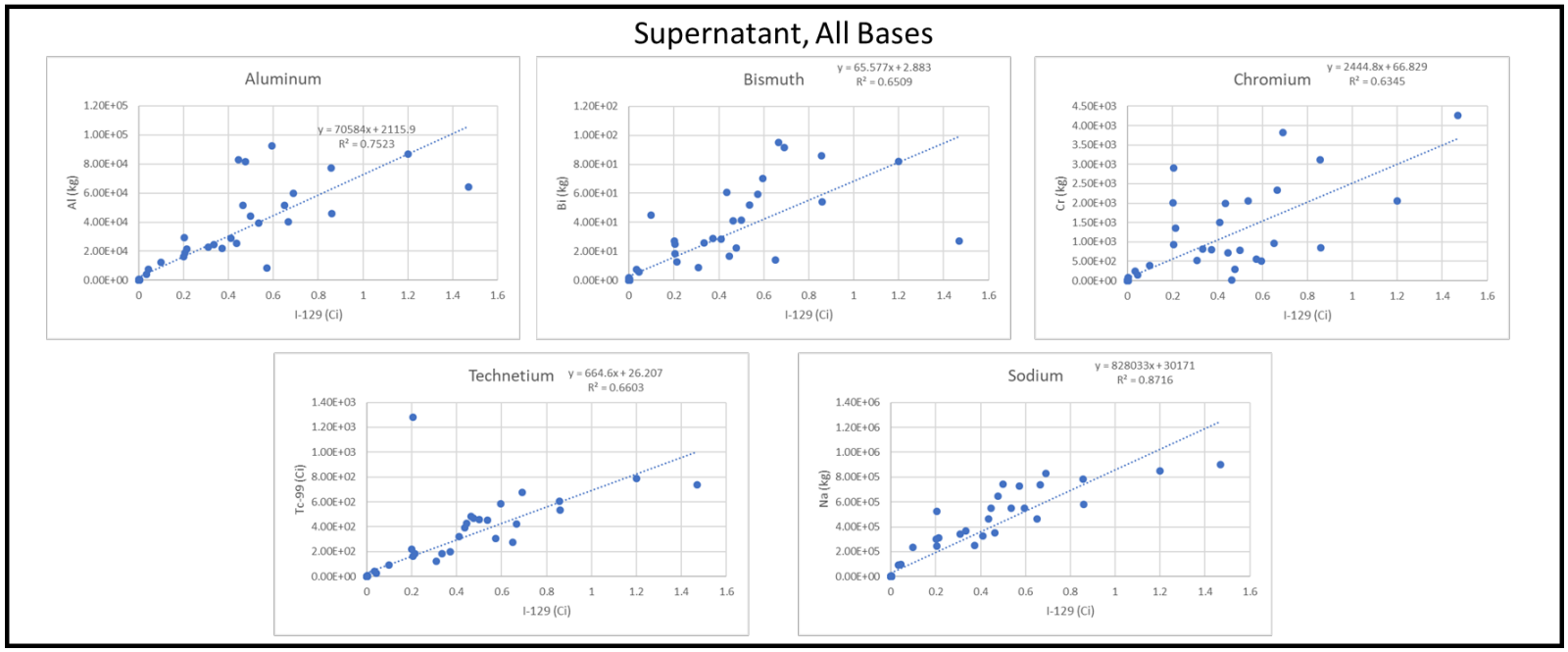

Figure A.2. Plots used to determine correlations between I-129 and specific elements in the supernatant and all inventory bases.

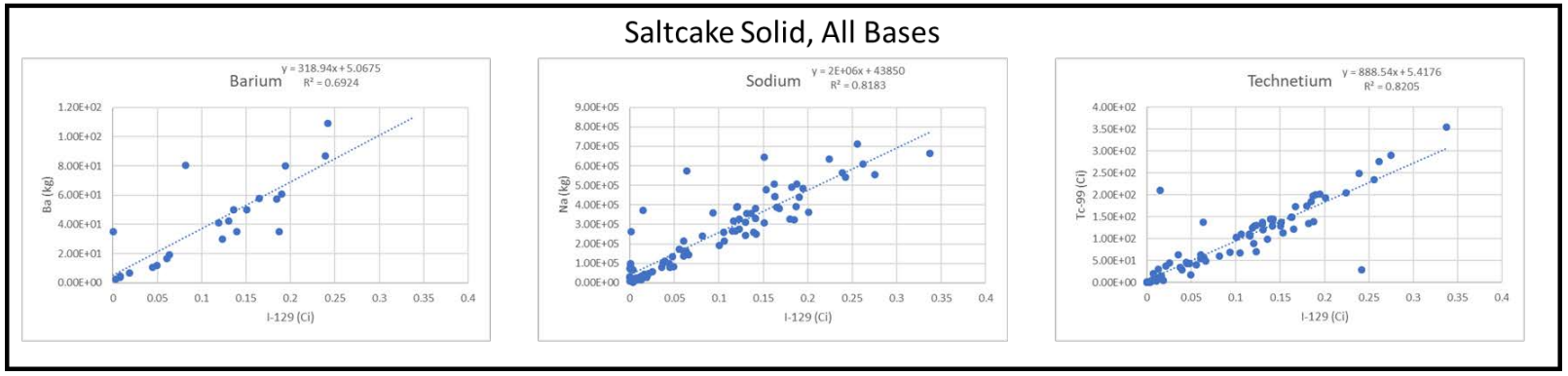

Figure A.3. Plots used to determine correlations between I-129 and specific elements in the saltcake solid and all inventory bases.

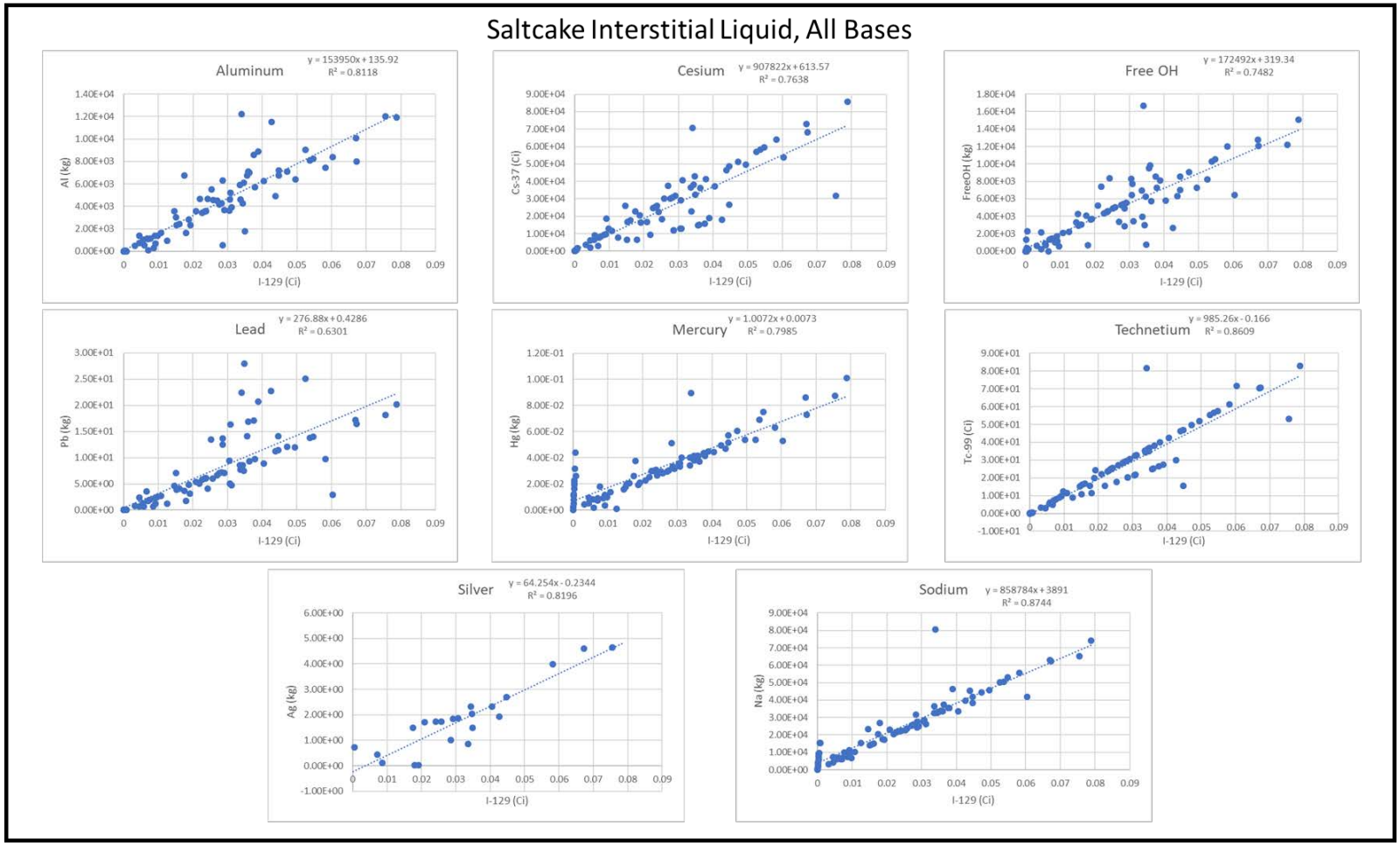

Figure A.4. Plots used to determine correlations between I-129 and specific elements in the saltcake interstitial liquid and all inventory bases.

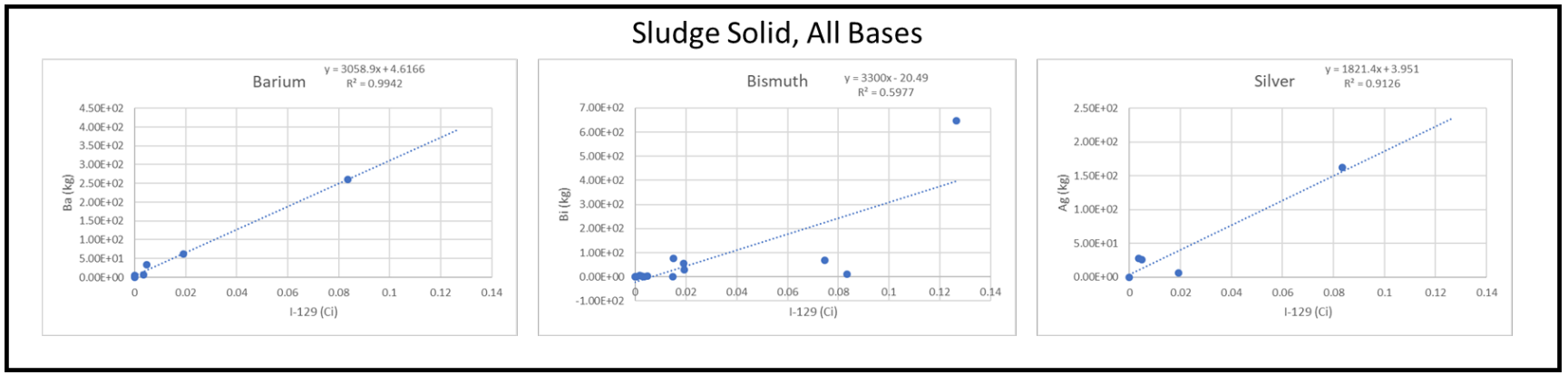

Figure A.5. Plots used to determine correlations between I-129 and specific elements in the sludge solid and all inventory bases.

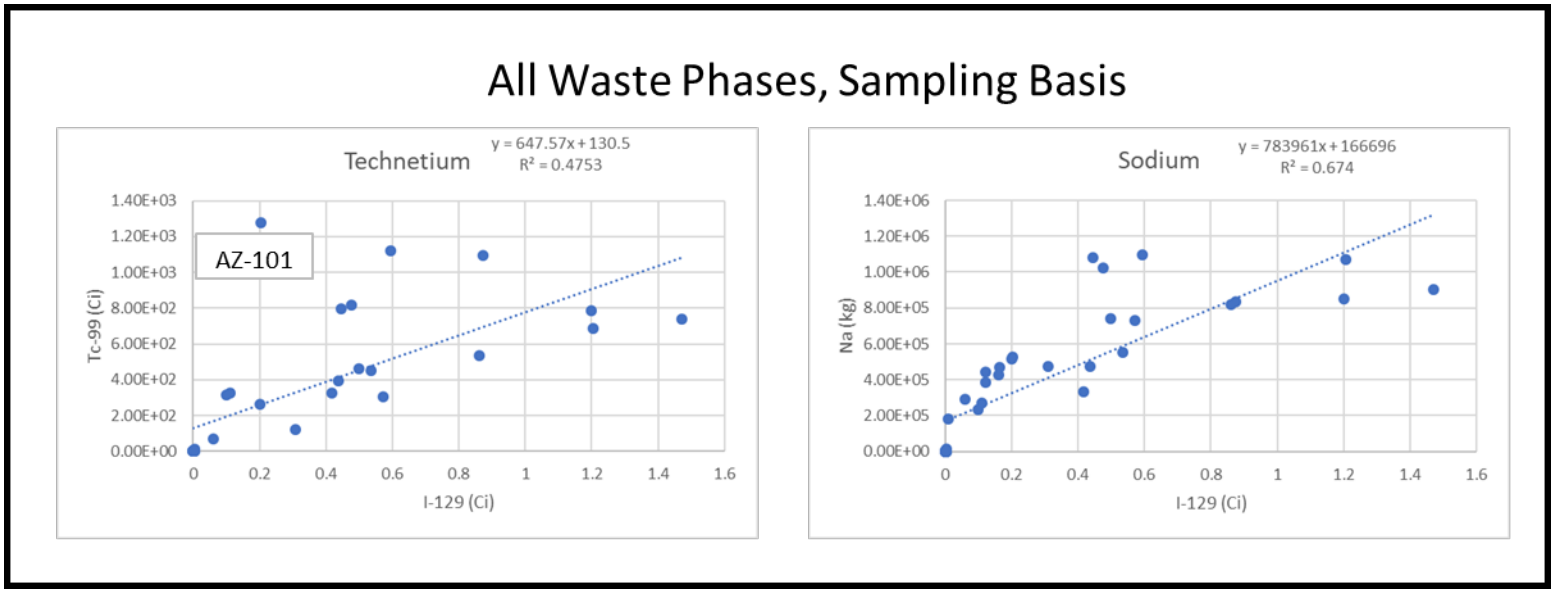

Figure A.6. Plots used to determine correlations between I-129 and specific elements in all waste phases and sampling basis data.

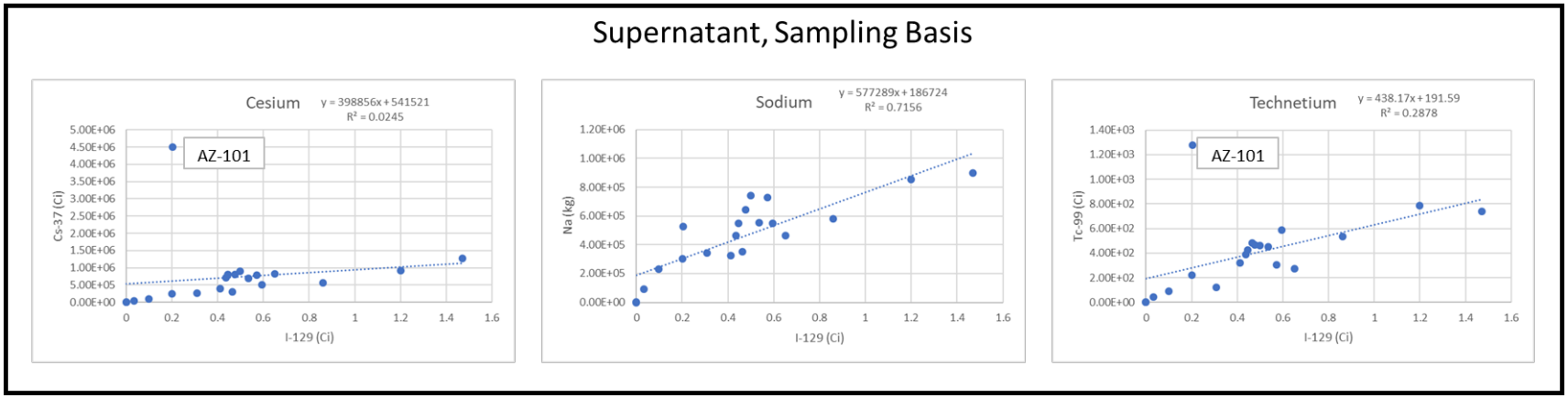

Figure A.7. Plots used to determine correlations between I-129 and specific elements in the supernatant and sampling basis data.

Appendix B – Correlation Plots for Projected Monthly Composition of the Liquid Tank Waste Fed to TSCR

The following are correlation plots for projected monthly composition of the liquid tank waste fed to TSCR based on the input file obtained from WRPS, titled “Monthly AP-107 to TSCR Feed Vector Crosstab CaseID 9157.xlsx” at publication date.

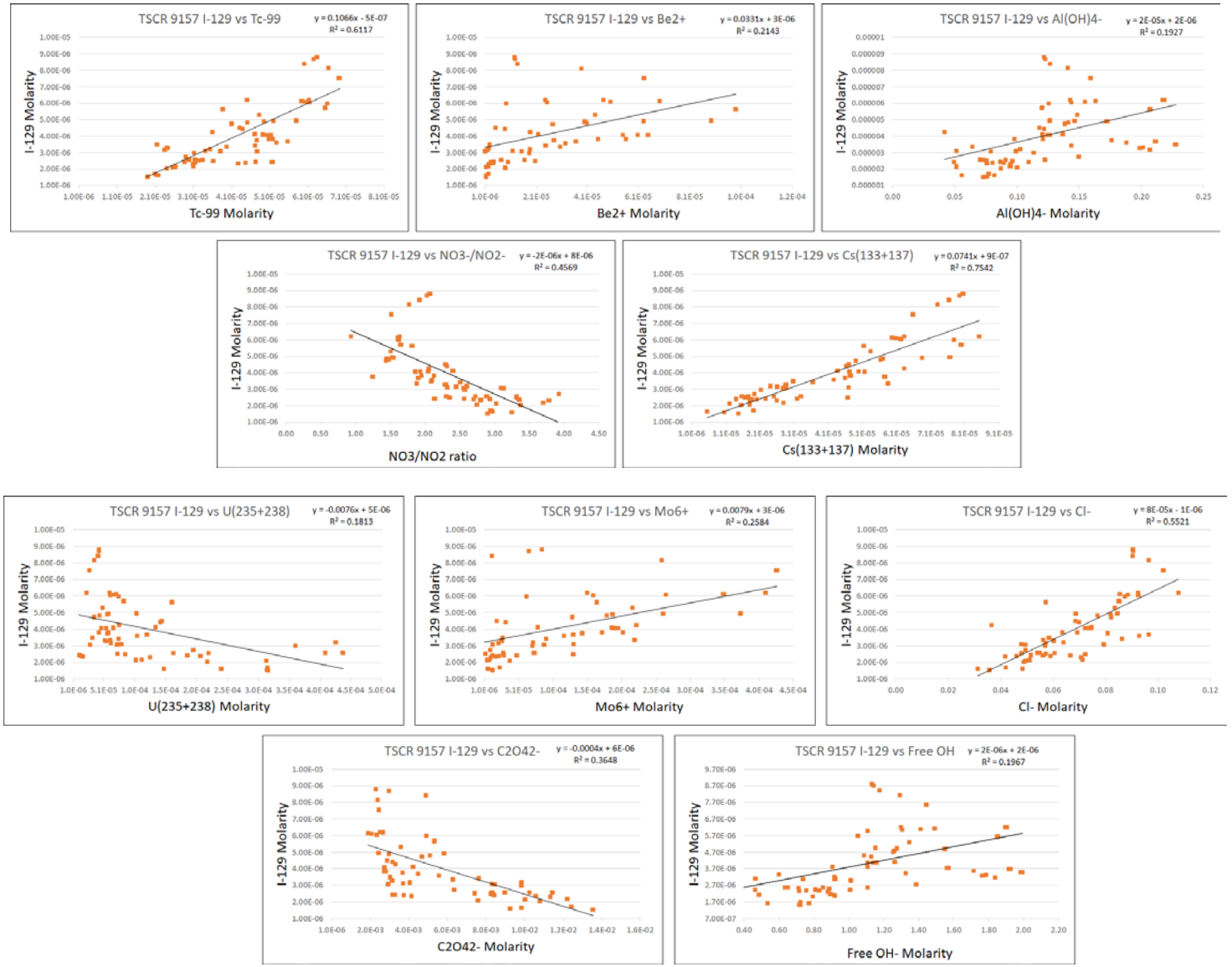

Figure B.1. Plots used to determine correlations between I-129 and specific elements in the TSCR feed for the entire campaign.

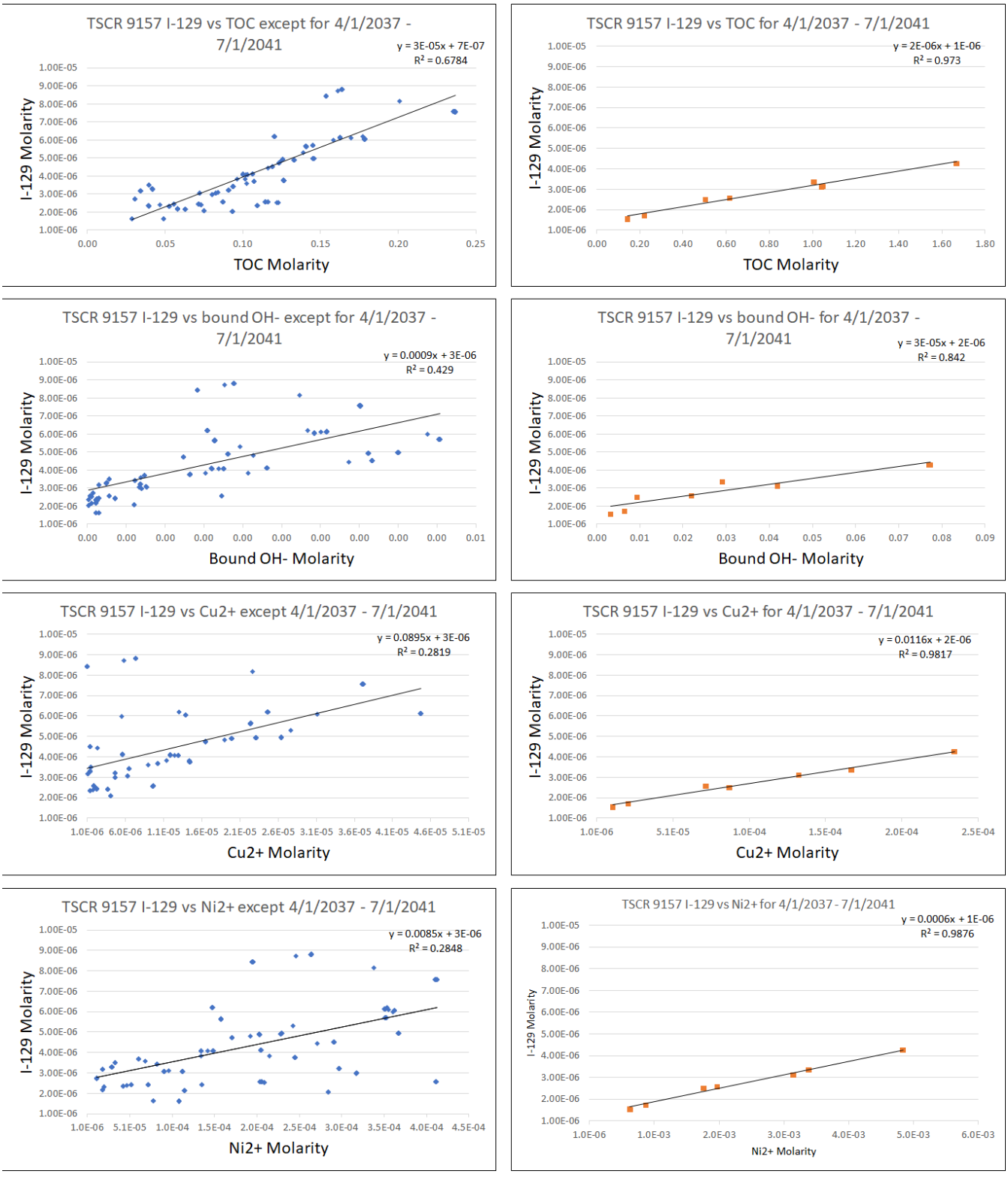

Figure B.2. Plots used to determine correlations between I-129 and specific elements in the TSCR feed with the input data for the 4/1/2037 - 7/1/2041 dates are separated into the individual subsets.

Distribution List

All distribution of the current report will be made electronically.

Washington River Protection Solutions
- Benson, PA
- Cree, LH
- Mabrouki, R
- Reynolds, JG
- Skeen, RS
- Swanberg, DJ
- Vitali, JR
- Wagnon, TJ
- WRPS Documents (TOCVND@rl.gov)

Pacific Northwest National Laboratory
- Arm, ST
- Asmussen, RM
- Bottenus, CLH
- Brouns, TM
- Fountain, MS
- Levitskaia, TG
- Peeler, DK
- Project File
- Information Release

Pacific Northwest National Laboratory

902 Battelle Boulevard
P.O. Box 999
Richland, WA 99354
1-888-375-PNNL (7665)

www.pnnl.gov